NACA RM L56I24

NACA

RESEARCH MEMORANDUM

WIND-TUNNEL INVESTIGATION OF THE AERODYNAMIC CHARACTERISTICS OF A SERIES OF SWEPT, HIGHLY TAPERED, THIN WINGS AT TRANSONIC SPEEDS

TRANSONIC-BUMP METHOD

By Albert G. Few, Jr., and Paul G. Fournier

Langley Aeronautical Laboratory
Langley Field, Va.

NATIONAL ADVISORY COMMITTEE
FOR AERONAUTICS

WASHINGTON

January 4, 1957
Declassified November 14, 1958

NACA RM L56I24

NATIONAL ADVISORY COMMITTEE FOR AERONAUTICS

RESEARCH MEMORANDUM

WIND-TUNNEL INVESTIGATION OF THE AERODYNAMIC CHARACTERISTICS OF A SERIES OF SWEPT, HIGHLY TAPERED, THIN WINGS AT TRANSONIC SPEEDS

TRANSONIC-BUMP METHOD

By Albert G. Few, Jr., and Paul G. Fournier

SUMMARY

An investigation by the transonic-bump method of the static longitudinal aerodynamic characteristics of a series of swept, highly tapered, thin wings has been made in the Langley high-speed 7- by 10-foot tunnel. The Mach number range extended from 0.60 to 1.16 with corresponding Reynolds numbers ranging from about 0.72×10^6 to 0.97×10^6. The angle-of-attack range was from -10° to approximately 34°.

In general, the lift and drag characteristics varied with changes in sweep and aspect ratio in essentially the manner expected on the basis of past research. The wings of smallest sweep (11.30°) provided the least change in lateral center of pressure with lift but the greatest change in longitudinal center of pressure with lift. Moderately large changes in lateral center of pressure are noted when the longitudinal changes in center of pressure are at a minimum. A boundary was established which separated highly tapered wings showing increasing stability with increasing lift from those showing decreasing stability with increasing lift. The boundary so established is defined by somewhat smaller values of sweep angle and aspect ratio than is the boundary established on the basis of a somewhat different criterion by Shortal and Maggin in NACA Technical Note 1093.

INTRODUCTION

In order to achieve maximum performance, particularly at transonic and supersonic speeds, it is important to utilize the thinnest airfoil sections that can be tolerated from structural considerations. Highly

tapered wings offer certain structural advantages over wings of less taper and, therefore, the airfoil-section thickness ratio normally can be reduced as the ratio of tip chord to root chord is reduced. The identification of plan forms with essentially linear wing-alone pitching-moment characteristics is an important phase in airplane design in that it provides a convenient basis for selecting the most appropriate wing to be used in conjunction with a desired tail location. From considerations of the wing-alone results presented in reference 1, wings having a zero sweep line within the region from about 0.75 to 1.00 chord in general appear to approach most closely a linear variation of pitching moment with lift while providing a desirable stabilizing tendency just before maximum lift.

The investigation of reference 1 covered a series of pointed wings of aspect ratio 4 and the same series of wings with tips clipped to give an aspect ratio of 3. The purpose of the present investigation was to extend the range of wing aspect ratio over that which was given in reference 1. Three basic pointed wings were chosen, each having an aspect ratio of 5 and NACA 65A003 airfoil sections. The sweep angle was varied to provide zero sweep lines at 0.50 chord, 0.75 chord, and 1.00 chord. Each wing was tested in its original zero-taper, aspect-ratio-5 condition as well as with the tips clipped to provide aspect ratios of 4 and 3 and taper ratios of 0.11 and 0.25, respectively.

The investigation utilized semispan models mounted on a transonic-bump in the Langley high-speed 7- by 10-foot tunnel.

The Mach number range extended from 0.60 to 1.16 with corresponding Reynolds numbers ranging from about 0.72×10^6 to 0.97×10^6. The results presented herein were derived from measurements of lift, drag, pitching moment, and root bending moment due to lift.

COEFFICIENTS AND SYMBOLS

C_L lift coefficient, $\dfrac{\text{Twice semispan lift}}{qS}$

C_D drag coefficient, $\dfrac{\text{Twice semispan drag}}{qS}$

$C_{D_{L=0}}$ minimum drag coefficient

C_m pitching-moment coefficient referred to $0.25\bar{c}$,

$$\frac{\text{Twice semispan pitching moment}}{qS\bar{c}}$$

C_B bending-moment coefficient due to lift about longitudinal stability axes, $\frac{\text{Bending moment}}{q\frac{S}{2}\frac{b}{2}}$

q effective dynamic pressure over span of wing, $\frac{\rho V^2}{2}$, lb/sq ft

q_a average chordwise local dynamic pressure, lb/sq ft

S twice area of semispan wing model, sq ft

A aspect ratio, b^2/S

$\bar{c}$ mean aerodynamic chord of wing, based on relationship $\frac{2}{S}\int_0^{b/2} c^2 dy$, ft

c local wing chord, ft

λ taper ratio

b twice span of semispan model, ft

y lateral distance from plane of symmetry, ft

ρ air density, slugs/cu ft

V free-stream velocity, ft/sec

M effective Mach number over span of wing

M_a average chordwise local Mach number

M_l local Mach number

α angle of attack, deg

$\Lambda_{c/4}$ wing sweep angle with respect to quarter-chord line, deg

y_{cp} lateral effective center-of-pressure location, $\frac{C_B}{C_L}$

x_{cp} longitudinal effective center-of-pressure location, $\left(0.25 - \frac{C_m}{C_L}\right)$

MODEL AND APPARATUS

The semispan wing models used in the investigation were constructed of steel to the dimensions given in figure 1. The models included a basic series of three wings all having an aspect ratio of 5, a taper ratio of 0, and NACA 65A003 airfoil sections parallel to the free stream with quarter-chord sweep angles of 11.30°, 21.80°, and 30.97° corresponding to zero-sweep lines at 0.50 chord, 0.75 chord, and 1.00 chord. The tips of each of the basic wings were clipped to give aspect ratios of 4 and 3 and taper ratios of 0.11 and 0.25, respectively.

A photograph of one of the models mounted on the bump in the Langley high-speed 7- by 10-foot tunnel is shown as figure 2. The wings were mounted on an electrical strain-gage balance which was enclosed in the bump and which measured the lift, drag, pitching moment, and root bending moment due to lift. A small gap existed between the wing root section and balance cover plate; however, use of a sponge-rubber seal at the base of the models minimized air leakage from within the balance chamber.

TESTS AND CORRECTIONS

The tests were made in the Langley high-speed 7- by 10-foot tunnel; an adaptation of the NACA wing-flow technique was used to obtain transonic speeds. The technique used in the present investigation involves mounting the wings in a high-velocity flow field (generated over the curved surface of a bump, located on the tunnel floor) and is identical to that used in reference 1.

Typical contours of local Mach number in the vicinity of the model location on the bump (obtained from surveys with no model in position), are shown in figure 3. Mach number variations of about 0.02 existed over the model semispan at the lowest Mach numbers and about 0.04 at the highest Mach numbers; whereas, the chordwise Mach number variations were generally less than 0.02. No attempt has been made to evaluate the effects of the spanwise and chordwise Mach number variations. The effective test Mach number was obtained from contour charts similar to those presented in figure 3 by using the relationship

$$M = \frac{2}{S}\int_0^{b/2} cM_a \, dy$$

Similarly, the effective dynamic pressure has been obtained from contour charts by using the relationship

$$q = \frac{2}{S}\int_0^{b/2} cq_a \, dy$$

Force and moment data were obtained for the wing-alone configurations through a Mach number range from 0.60 to 1.16, which corresponds to a Reynolds number range from about 0.72×10^6 to 0.97×10^6. The angle of attack varied from about -10° to a maximum of approximately 34°.

Jet-boundary corrections have not been evaluated, since the boundary conditions to be satisfied are not rigorously defined. However, inasmuch as the effective flow field is large in comparison with the span and chord of the wings, the corrections are believed to be small. No attempt has been made to correct the data for aeroelastic distortion; however, a rough estimate of the model flexibility indicated that aeroelastic effects should be small.

RESULTS AND DISCUSSION

Presentation of Results

Aerodynamic characteristics of the series of swept, highly tapered, thin wings having aspect ratios of 5, 4, and 3 are presented as follows:

Basic data:

	Figure
α against C_L; $\Lambda_{c/4} = 11.30^\circ$	4
α against C_L; $\Lambda_{c/4} = 21.80^\circ$	5
α against C_L; $\Lambda_{c/4} = 30.97^\circ$	6
C_D against C_L; $\Lambda_{c/4} = 11.30^\circ$	7
C_D against C_L; $\Lambda_{c/4} = 21.80^\circ$	8
C_D against C_L; $\Lambda_{c/4} = 30.97^\circ$	9
C_m against C_L; $\Lambda_{c/4} = 11.30^\circ$	10
C_m against C_L; $\Lambda_{c/4} = 21.80^\circ$	11
C_m against C_L; $\Lambda_{c/4} = 30.97^\circ$	12
C_B against C_L; $\Lambda_{c/4} = 11.30^\circ$	13
C_B against C_L; $\Lambda_{c/4} = 21.80^\circ$	14
C_B against C_L; $\Lambda_{c/4} = 30.97^\circ$	15
Summary of aerodynamic characteristics	16-21

A brief discussion based primarily on the summary data of figures 16 to 21 is presented herein. The slopes presented in the summary figures have been averaged over a lift-coefficient range of ± 0.10. In order to facilitate presentation of the data, staggered scales have been used in many of the figures and care should be taken in identifying the zero axis for each curve.

Lift and Drag Characteristics

Examination of figure 16 reveals certain general trends with respect to the effects of wing plan form on lift-curve slope which are well known. The lift-curve slope was reduced by either a reduction in aspect ratio or an increase in sweep. It will be noted, however, that the change in aspect ratio from 5 to 4 was much less significant than the change from 4 to 3.

Results presented in figure 16 indicate that clipping the wing tips to obtain reductions in aspect ratio had, in general, little effect on the overall minimum drag characteristics through the range of Mach number. However, a favorable sweep effect is noted in that decreases in the minimum drag through the transonic speed range are obtained. Also shown in figure 16 are the effects of sweep and aspect-ratio reductions on the variation of the drag-due-to-lift parameter with Mach number. As would be expected, values of the drag-due-to-lift parameter $\frac{\partial C_D}{\partial C_L{}^2}$ generally were somewhat higher when the aspect ratio was reduced. Effects of sweep, at least for the sweep range investigated, generally were small throughout the Mach number range.

Comparisons of lift-drag ratios varying with lift coefficient are shown in figure 17 for Mach numbers of 0.90 and 1.10. No very significant advantages are noted with regard to sweep for either Mach number; however, some reductions are evidenced when the aspect ratio is reduced. In general, these reductions in lift-drag ratios with reduced aspect ratio occur throughout the range of lift coefficient for both a Mach number of 0.90 and 1.10. Maximum values of lift-drag ratios for a Mach number of 1.10 are considerably less than those at subsonic speeds.

Longitudinal Stability Characteristics

Any large change in the linearity of the pitching-moment curves is undesirable especially if the change is in an unstable direction. In order to study to some extent the degree to which this linearity in the pitching-moment curves is affected by wing plan form, some comparisons

of the effects of wing plan form on the overall shape of the pitching-moment curves are shown in figure 18. These curves, for three representative Mach numbers, have been lifted from the basic data (figs. 4 to 15) and are presented here for a more direct comparison of the effects of sweep and aspect-ratio reductions. At Mach numbers of 0.80 and 0.90, aspect-ratio reductions of the more highly swept wings ($\Lambda_{c/4} = 21.80^\circ$ and $\Lambda_{c/4} = 30.97^\circ$) were more significant than aspect-ratio reductions of the wings with least sweep ($\Lambda_{c/4} = 11.30^\circ$), especially in the moderate range of lift coefficient where the unstable changes in pitching-moment curves were generally reduced. For the case of wings of low sweep ($\Lambda_{c/4} = 11.30^\circ$), no significant changes in the linearity of the pitching-moment curves were noted when the aspect ratio was reduced; however, a reduction in static margin $\frac{\partial C_m}{\partial C_L}$ occurred at low-lift coefficients, which was also noted for the higher sweep cases. It will be noted that the wings with less sweep (particularly $\Lambda_{c/4} = 11.30^\circ$) exhibit quite abrupt stable changes in longitudinal stability in a moderate lift-coefficient range, which are of significance since undesirable trim changes and maneuvering characteristics would likely be associated with a configuration having this type of pitching-moment behavior. The pitching-moment-curve nonlinearity noted for Mach numbers of 0.80 and 0.90 for the sweep range investigated generally did not occur at higher speeds, and the aspect-ratio reductions were of little importance as Mach number increased to 1.10.

In order to provide some generalization of the effects of geometric variables on the linearity of the pitching-moment curves of highly tapered wings ($\lambda = 0$ to 0.30), the present results and those of references 1 and 2 have been interpreted in terms of the relation of the wings to a boundary which separates plan forms that become increasingly stable as lift is increased from those that become decreasingly stable as lift is increased. The resulting correlation (fig. 19) is given in terms of aspect ratio and quarter-chord sweep angle in the manner adopted by Shortal and Maggin in their well-known correlation given in reference 3. The criterion used in establishing the present boundary, however, differs from that used by Shortal and Maggin who separated the plan forms on the basis of stabilizing or destabilizing tendencies of the pitching-moment curves in the vicinity of maximum lift. The present criterion considers deviations of the pitching-moment curve at any positive lift coefficient below maximum lift from its slope at zero lift (fig. 19). If at any lift coefficient within the specified range the slope $\frac{\partial C_m}{\partial C_L}$ is less negative than at zero lift, the plan form is indicated by a solid symbol; whereas, if $\frac{\partial C_m}{\partial C_L}$ at positive lift is always more negative than at zero lift, the plan form is indicated by an open symbol. The boundary

separating these stability characteristics thereby defines plan forms having essentially linear pitching-moment characteristics. Such a boundary provides a convenient basis for the selection of plan forms most readily adaptable to airplanes with high or low tail locations or to tailless airplanes. The boundary obtained is considered applicable, however, only to taper ratios in the range considered herein - that is, between taper ratios of 0 and 0.30. Note that plan forms on the stable side of the present boundary are defined by more restricted ranges of sweep angle and aspect ratio than are the plan forms on the stable side of the Shortal-Maggin boundary.

The variation of the aerodynamic center with Mach number as affected by sweep and aspect ratio is shown in figure 20. The effect of aspect-ratio reduction is to shift the aerodynamic center forward a rather constant amount throughout the Mach number range without much effect on the overall variation with Mach number for a given sweep angle. The sweep effect noted is generally consistent with past results inasmuch as the maximum rearward shift of the aerodynamic center from subsonic to supersonic speeds is somewhat reduced as sweep angle increases.

In order to illustrate some trends in changes with lift coefficient of the locations of the effective longitudinal and lateral centers of pressure, data for Mach numbers of 0.90 and 1.10 are presented in figure 21. The centers of pressure will be referred to as effective centers of pressure, inasmuch as the lateral effective center of pressure was obtained by division of the root bending moment due to lift by the lift and the longitudinal effective center of pressure was obtained by division of the pitching moment by the lift. The changes in both longitudinal and lateral effective center-of-pressure location with lift coefficient (for all sweep angles investigated) at a Mach number of 1.10 are considerably smaller than changes at a Mach number of 0.90. The wing plan form which provides the least change with lift coefficient in longitudinal effective center-of-pressure location experiences considerable inward shifts with lift coefficient in the lateral effective center of pressure for either Mach number (fig. 21(c)). As pointed out in reference 1, such inward shifts are associated with tip separation. Clipping the tips generally relieves to some extent this inward movement of the lateral effective center of pressure with lift coefficient for both Mach numbers, but it also results in somewhat increased overall variation of the longitudinal effective center-of-pressure location with lift coefficient. The wing plan form which provides the least change in the lateral effective center-of-pressure location with lift coefficient also experiences the greatest change in the longitudinal effective center-of-pressure location (fig. 21(a)). This effect was also noted for the investigation of the highly tapered wings reported in reference 1. Moderately large changes in the lateral center of pressure are noted when the longitudinal changes in center of pressure are at a minimum.

CONCLUSIONS

Results of an investigation, by the transonic-bump method, of the static longitudinal aerodynamic characteristics of a series of highly tapered thin wings with varying degrees of sweep and different aspect ratios, obtained by clipping the tips of the basic pointed wings, indicate the following conclusions:

1. In general, the lift and drag characteristics varied with changes in sweep angle and aspect ratio in essentially the manner expected on the basis of previous research.

2. The wings of smallest sweep (11.30°) provided the smallest changes in lateral center of pressure with increasing lift, but the greatest changes in longitudinal center of pressure with increasing lift. Moderately large changes in lateral center of pressure are noted when the longitudinal changes in center of pressure are at a minimum.

3. A boundary was established which separates highly tapered wings showing increasing stability with increasing lift from those showing decreasing stability with increasing lift. The boundary so established is defined by somewhat smaller values of sweep angle and aspect ratio than is the boundary established on the basis of a somewhat different criterion by Shortal and Maggin in NACA Technical Note 1093.

Langley Aeronautical Laboratory,
National Advisory Committee for Aeronautics,
Langley Field, Va., August 31, 1956.

REFERENCES

1. Few, Albert G., Jr., and Fournier, Paul G.: Effects of Sweep and Thickness on the Static Longitudinal Aerodynamic Characteristics of a Series of Thin, Low-Aspect-Ratio, Highly Tapered Wings at Transonic Speeds - Transonic-Bump Method. NACA RM L54B25, 1954.

2. Emerson, Horace F.: Wind-Tunnel Investigation of the Effect of Clipping the Tips of Triangular Wings of Different Thickness, Camber, and Aspect Ratio - Transonic Bump Method. NACA TN 3671, 1956. (Supersedes NACA RM A53L03.)

3. Shortal, Joseph A., and Maggin, Bernard: Effect of Sweepback and Aspect Ratio on Longitudinal Stability Characteristics of Wings at Low Speeds. NACA TN 1093, 1946.

A	S, sq ft (twice semispan)	λ	$\bar{c}$, ft
5	0.1388	0	0.222
4	0.1372	0.11	0.225
3	0.1302	0.25	0.233

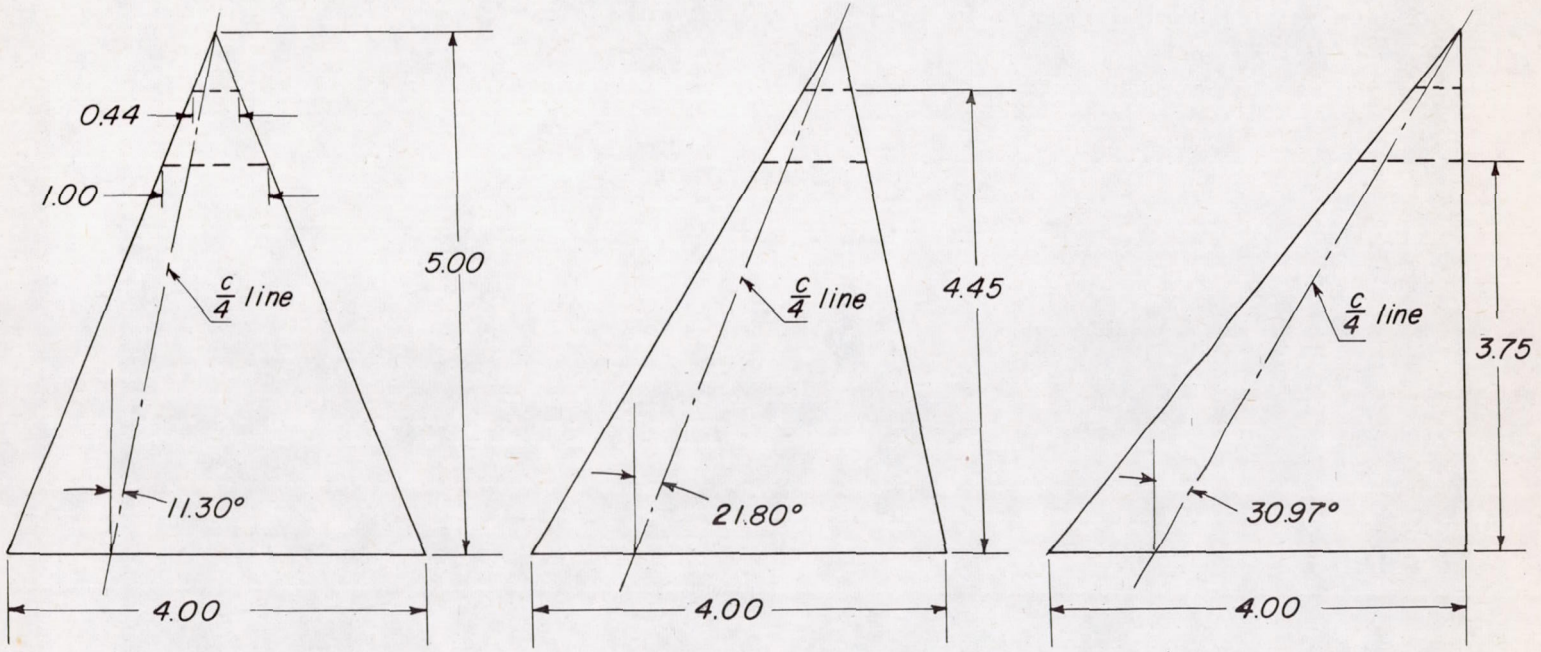
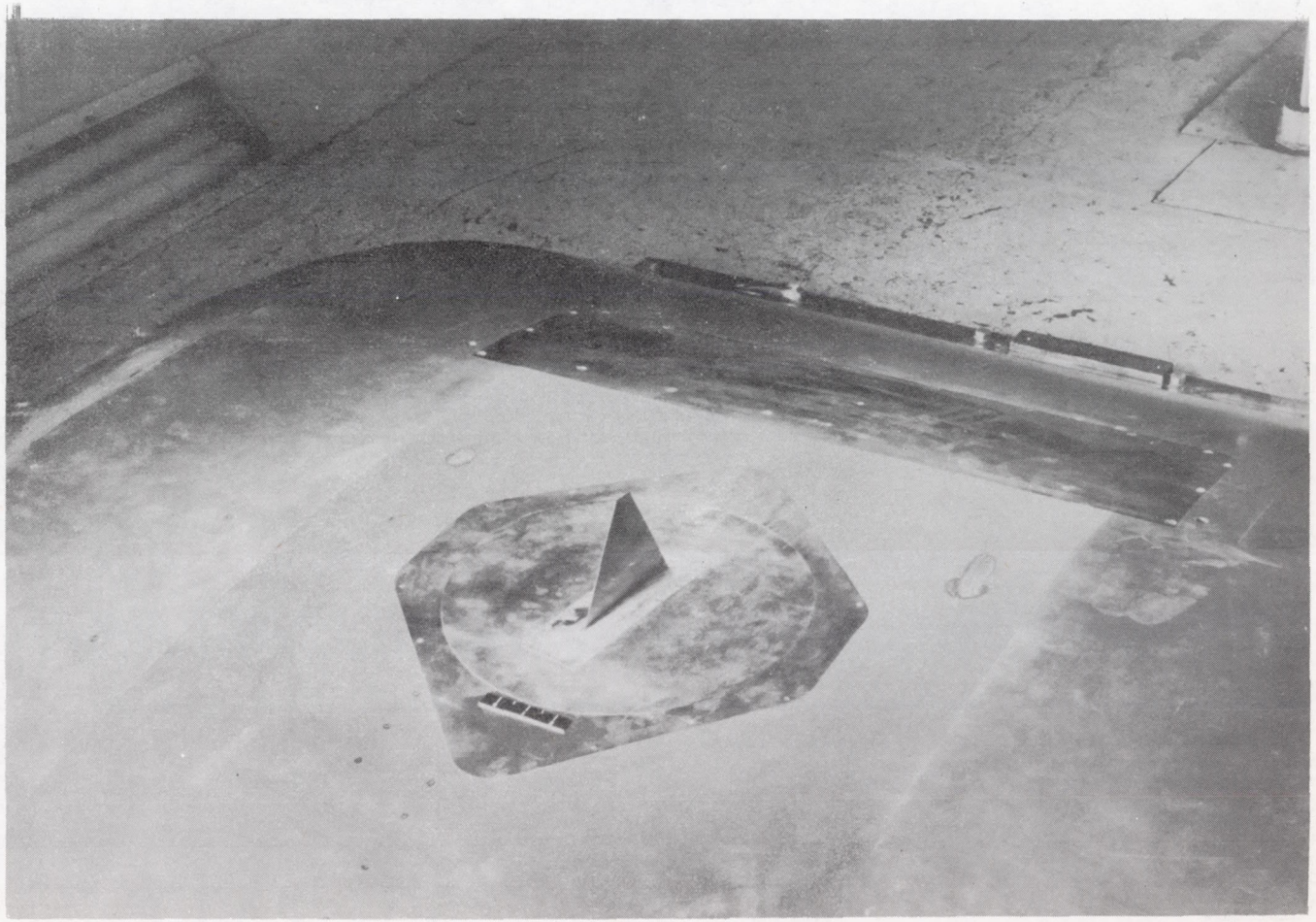


Figure 1.- Geometric characteristics of the test models. (All dimensions are in inches unless otherwise stated.)



L-76833.1

Figure 2.- Typical wing mounted on transonic bump in the Langley high-speed 7- by 10-foot tunnel.

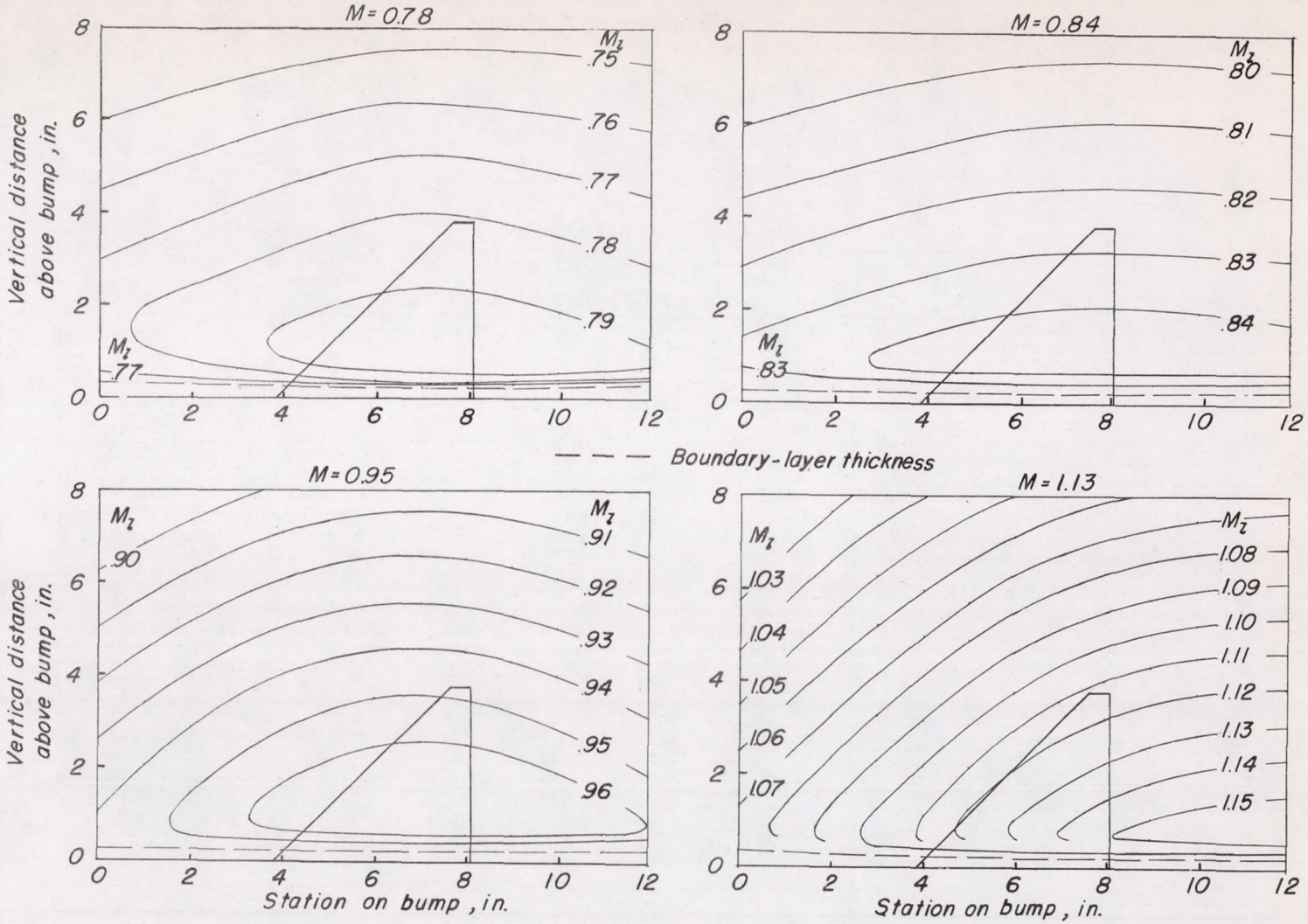
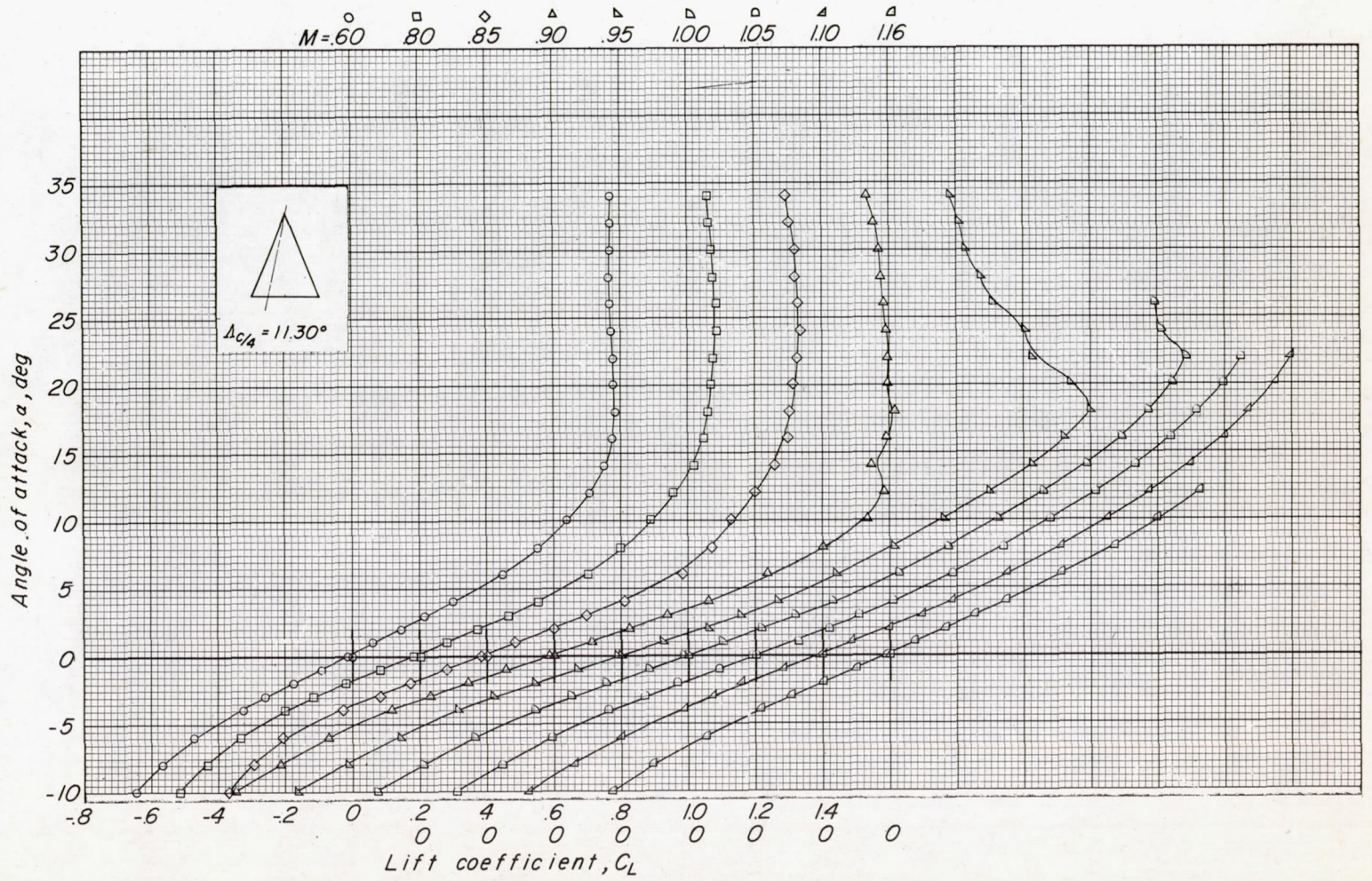
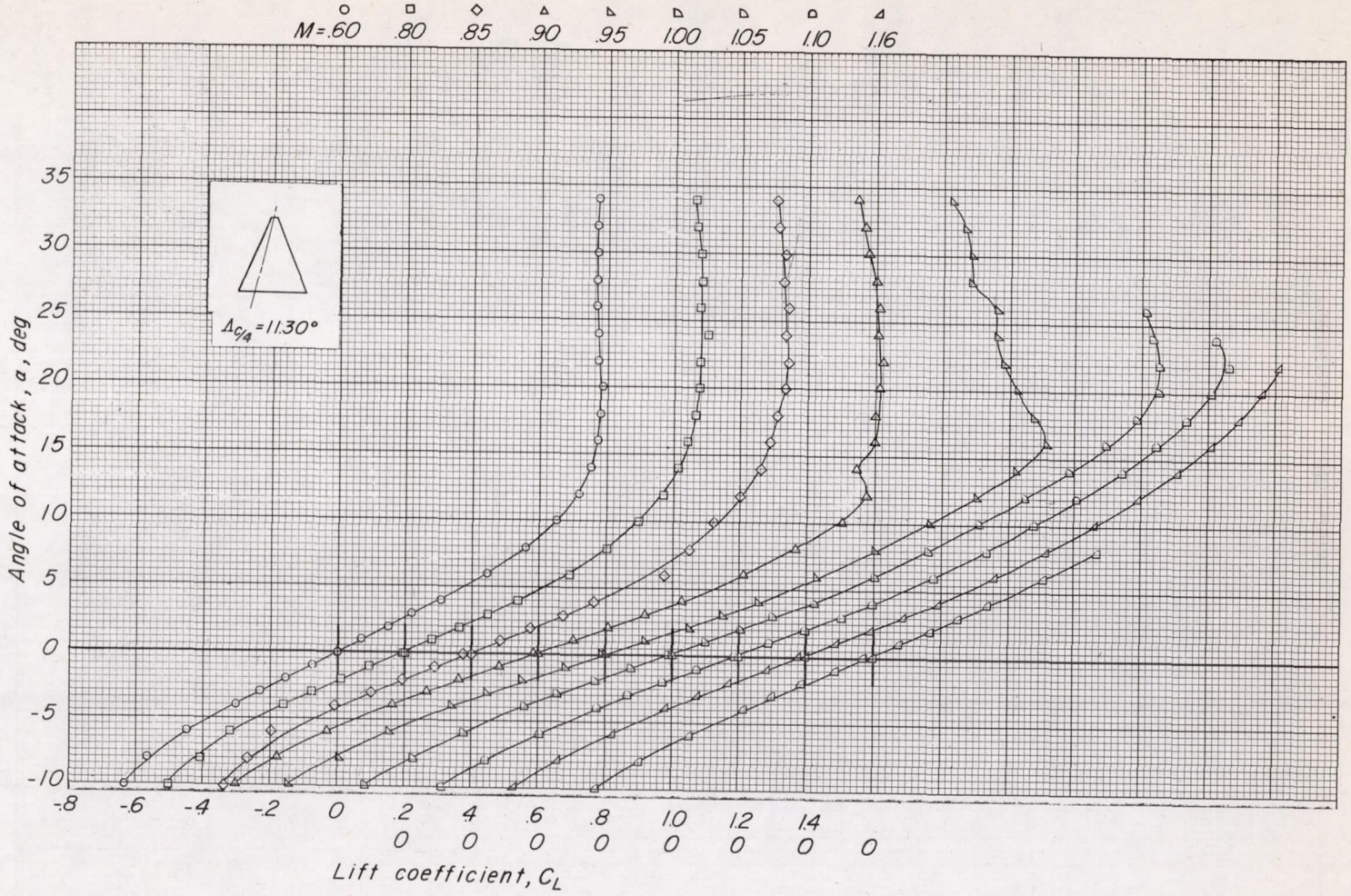


Figure 3.- Typical Mach number contours over transonic bump in region of model location.



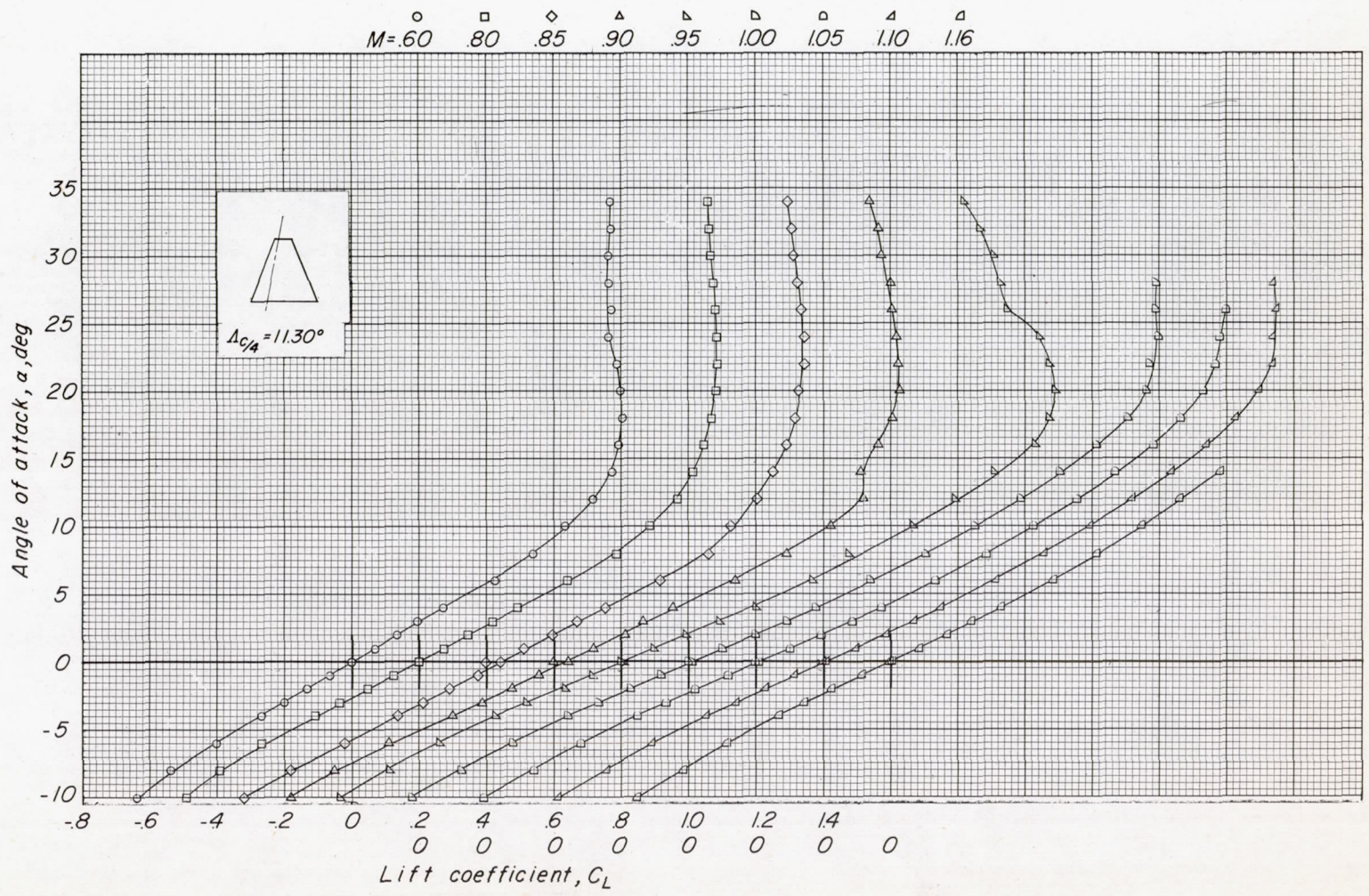
(a) A = 5.

Figure 4.- Variation of angle of attack with lift coefficient; $\Lambda_{c/4} = 11.30^{\circ}$.



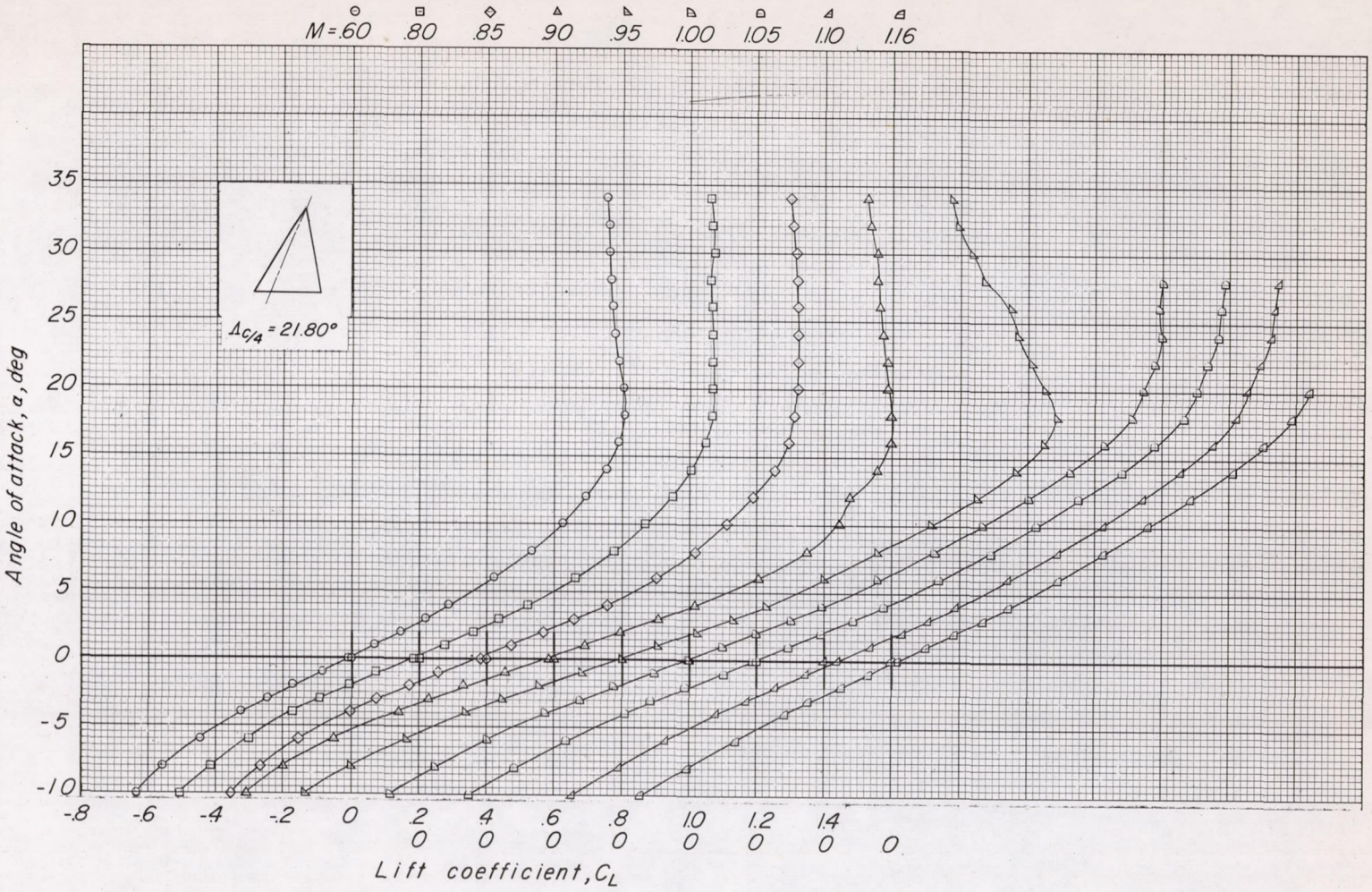
(b) A = 4.

Figure 4.- Continued.



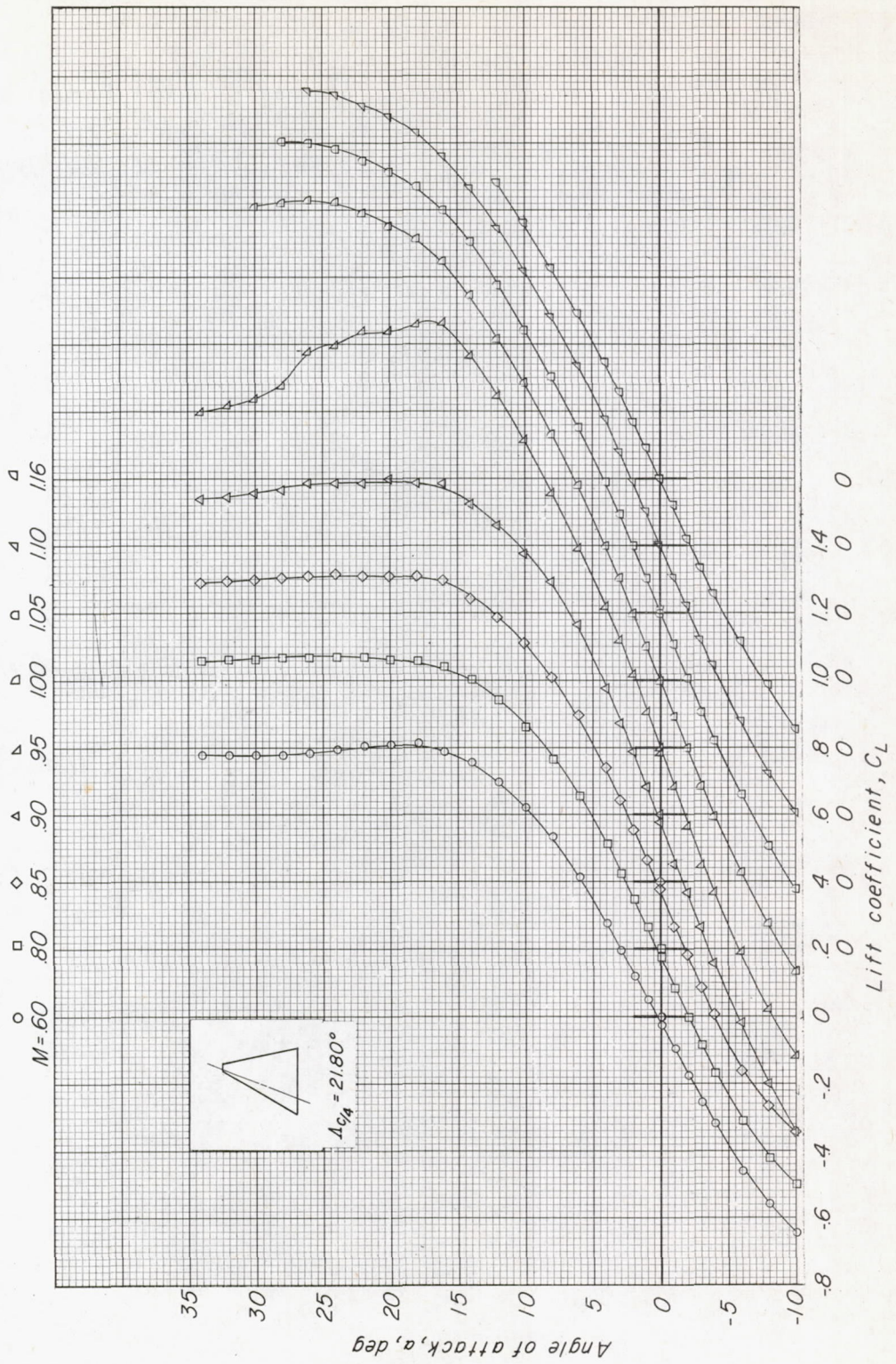
(c) A = 3.

Figure 4.- Concluded.



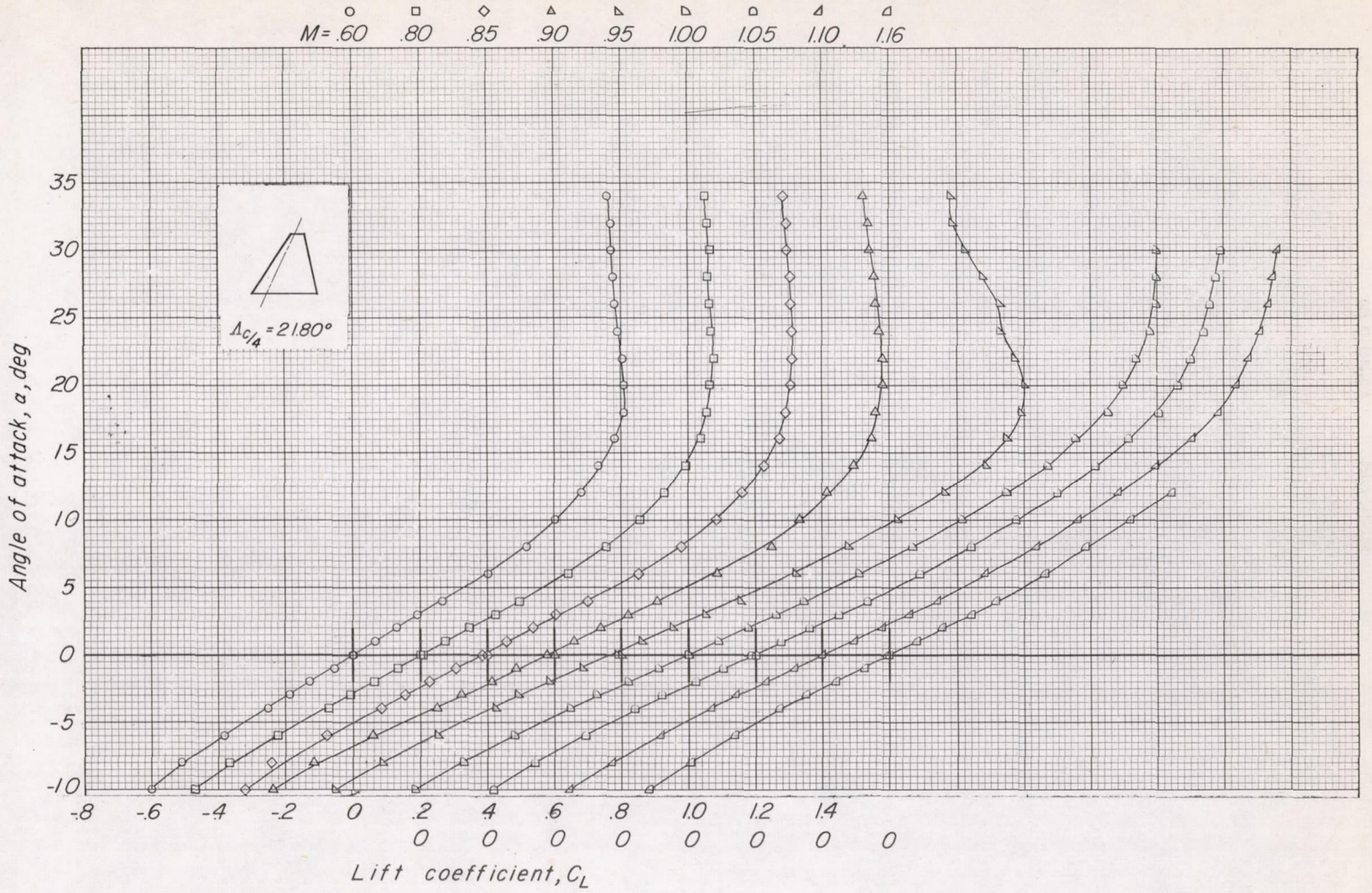
(a) A = 5.

Figure 5.- Variation of angle of attack with lift coefficient; $\Lambda_{c/4}$ = 21.80°.



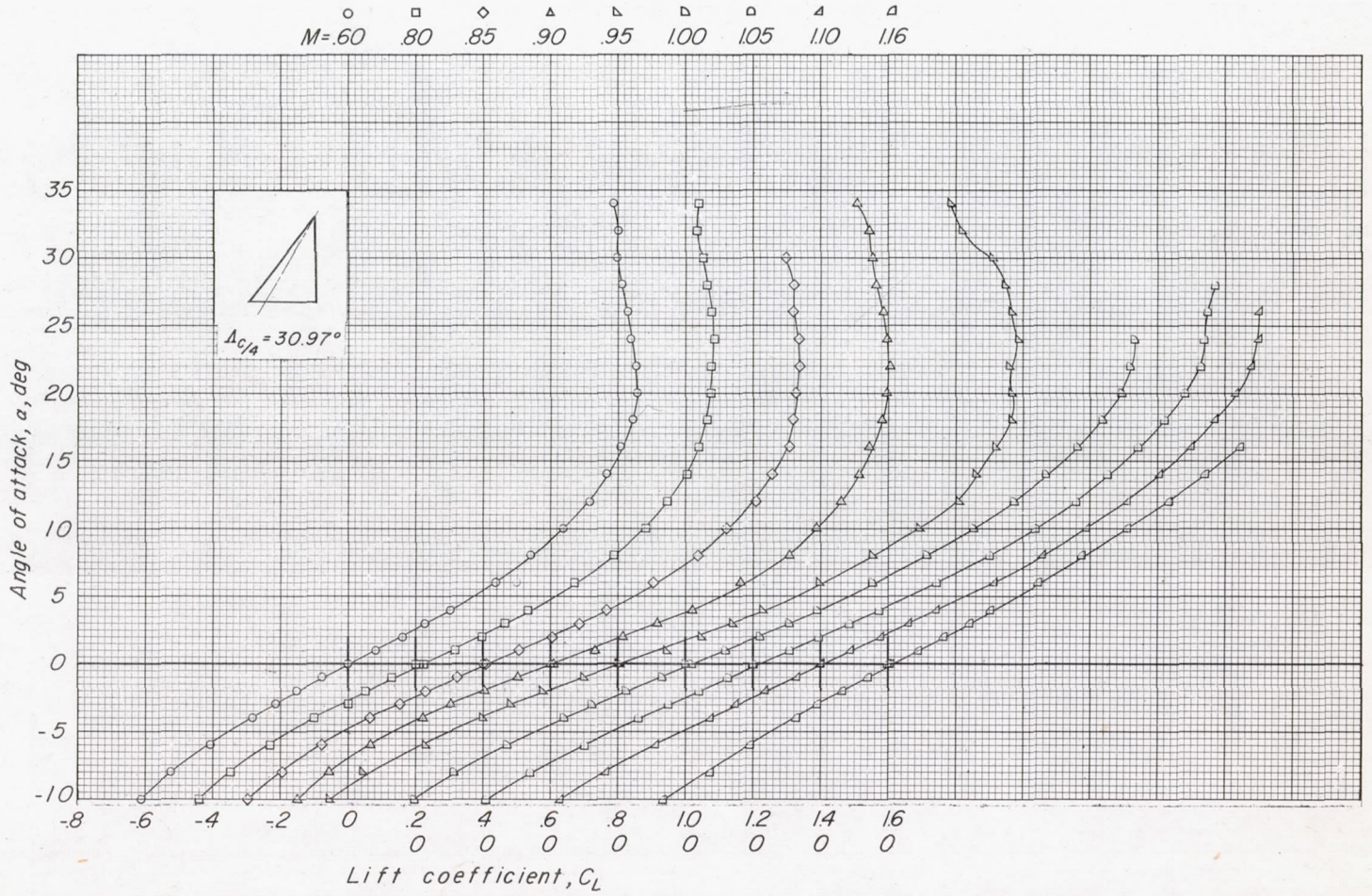
(b) A = 4.

Figure 5.- Continued.



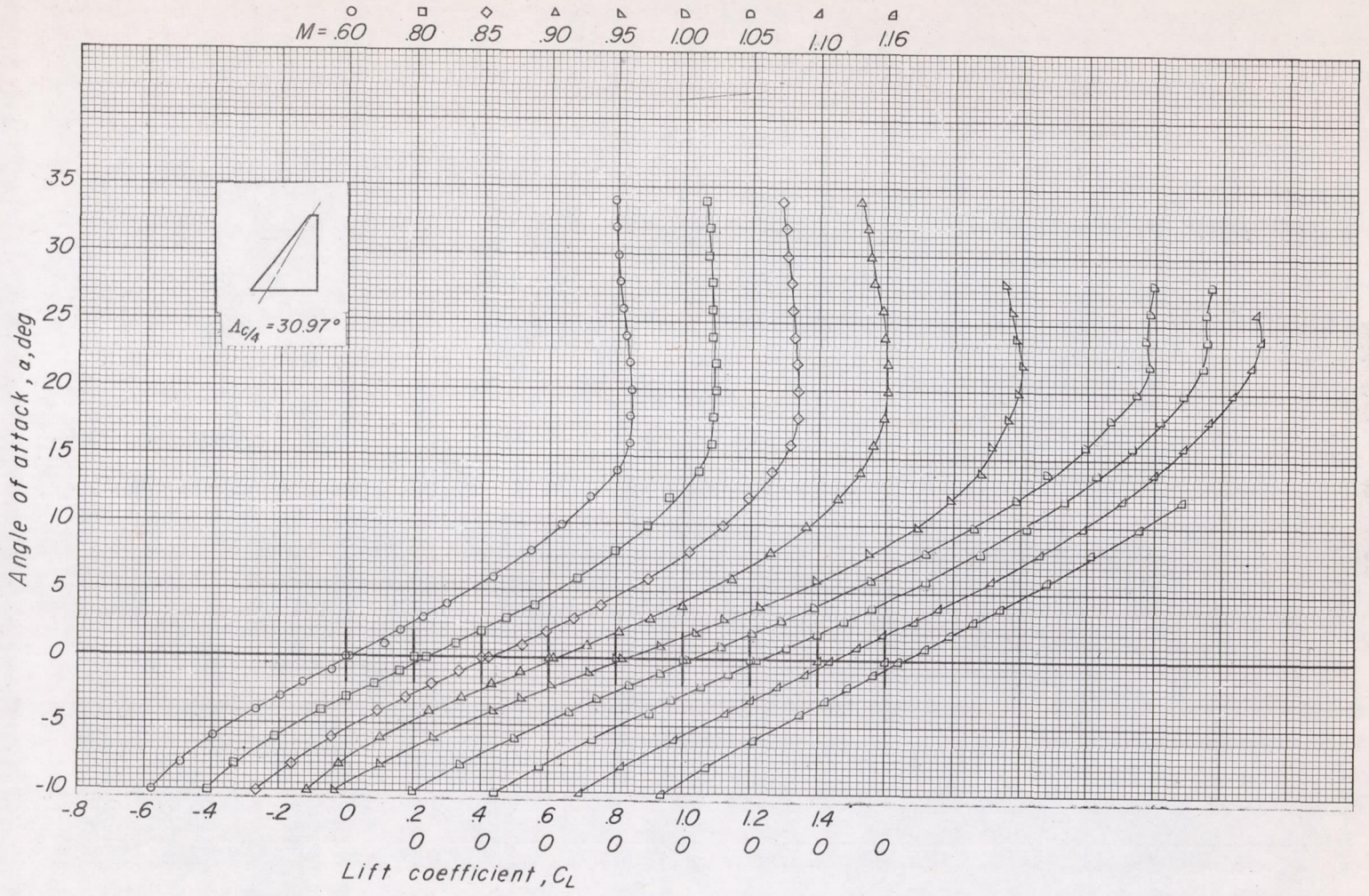
(c) A = 3.

Figure 5.- Concluded.



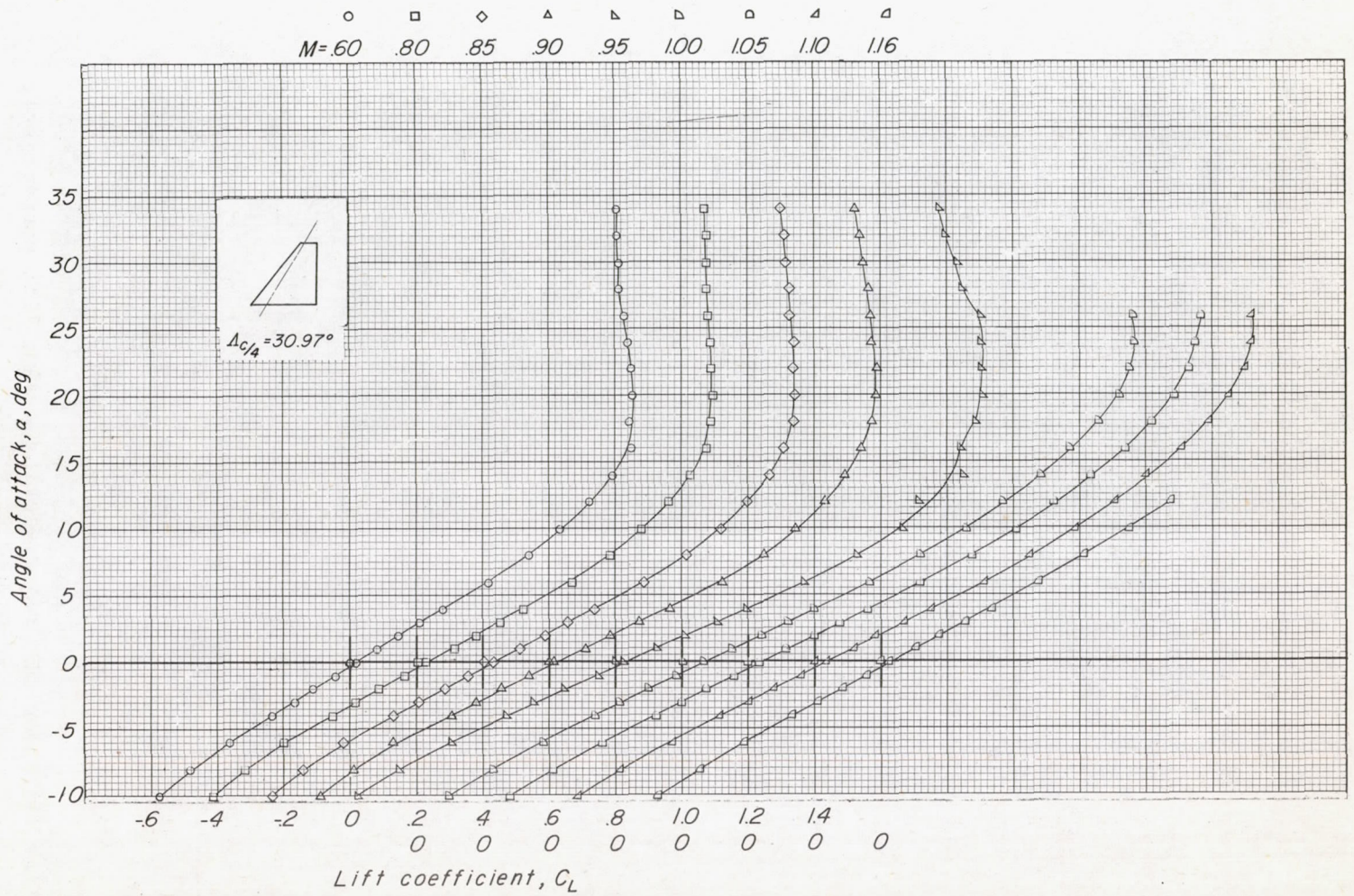
(a) A = 5.

Figure 6.- Variation of angle of attack with lift coefficient; $\Lambda_{c/4} = 30.97^{\circ}$.



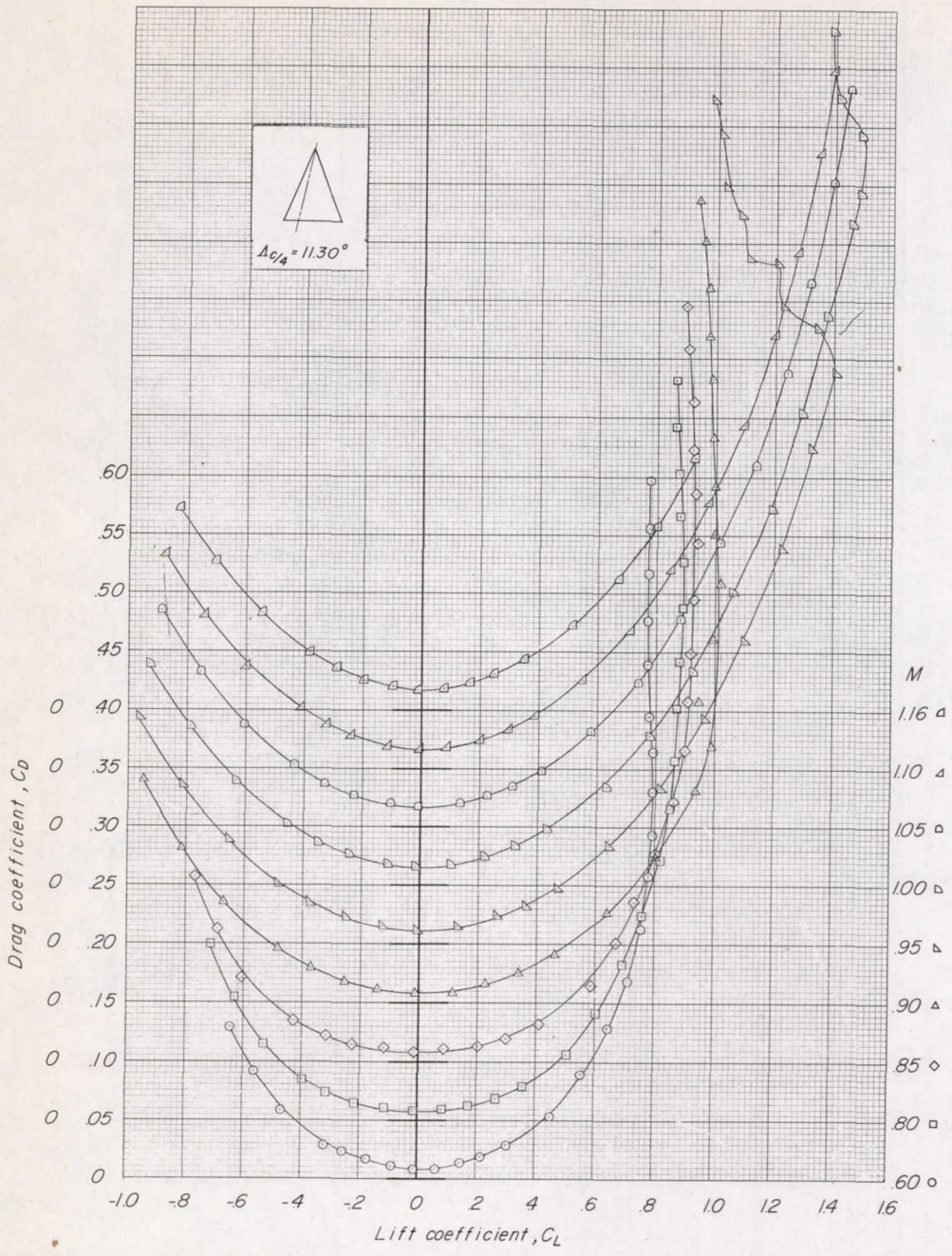
(b) A = 4.

Figure 6.- Continued.



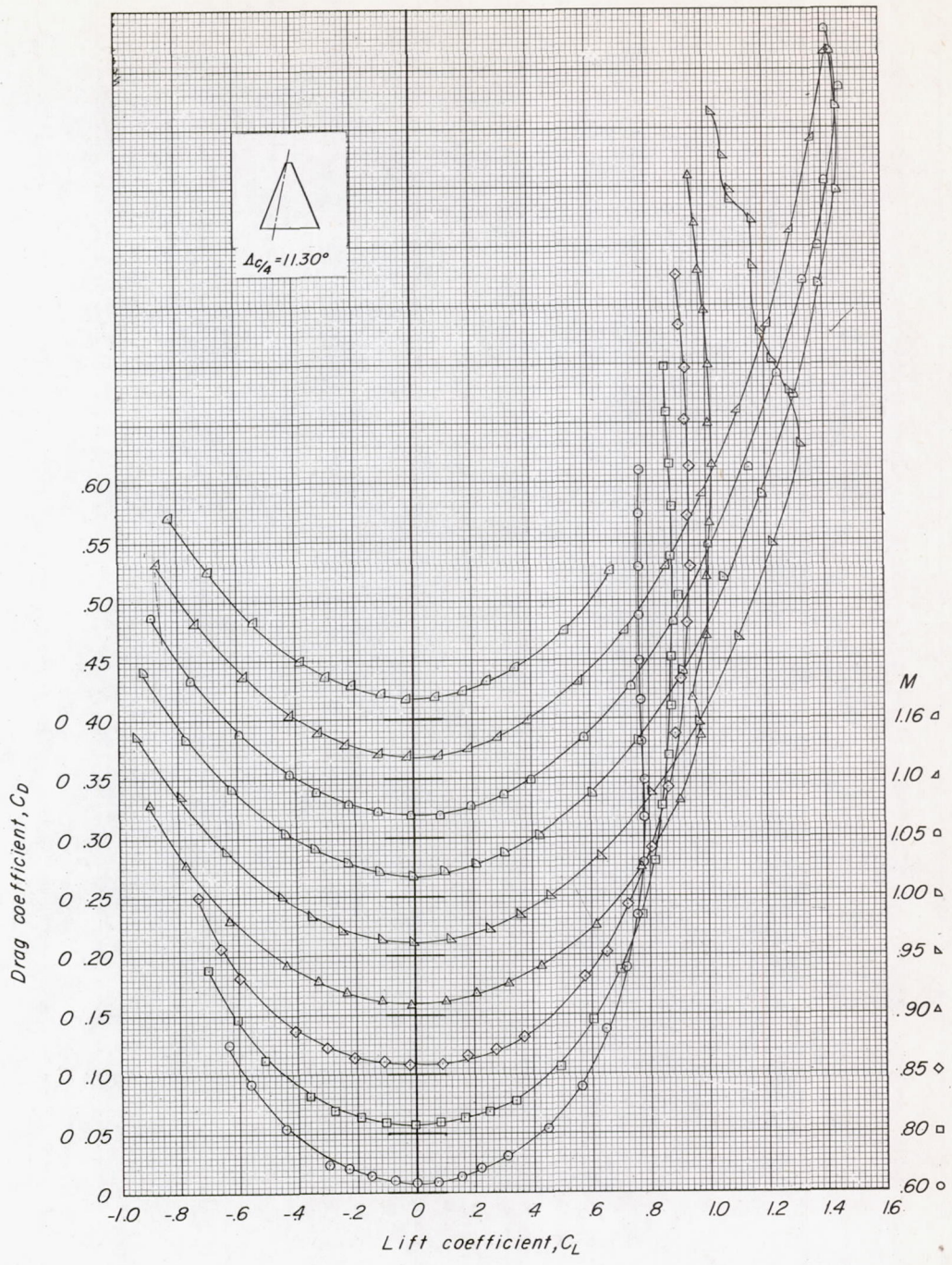
(c) A = 3.

Figure 6.- Concluded.



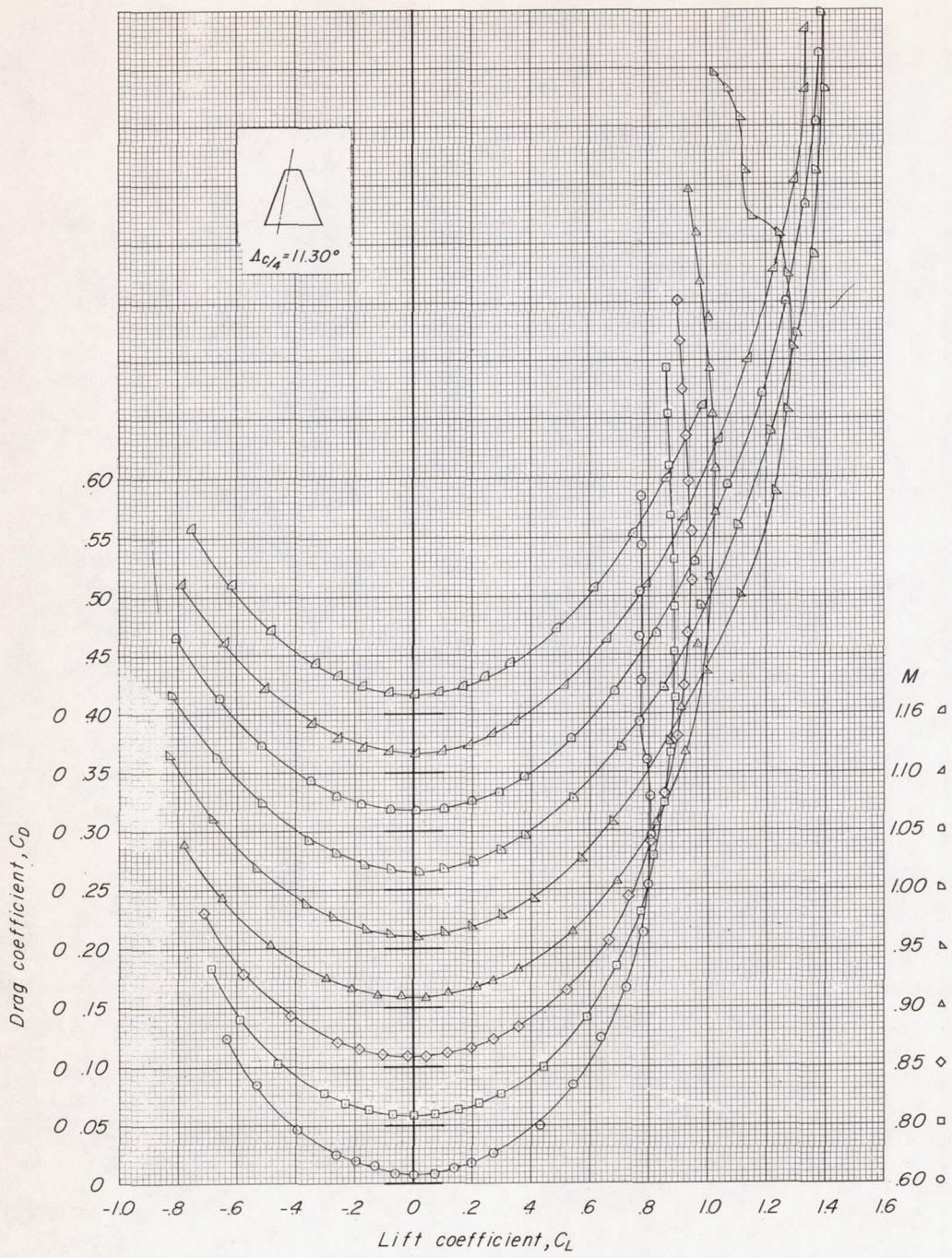
(a) A = 5.

Figure 7.- Variation of drag coefficient with lift coefficient; $\Lambda_{c/4}$ = 11.30°.



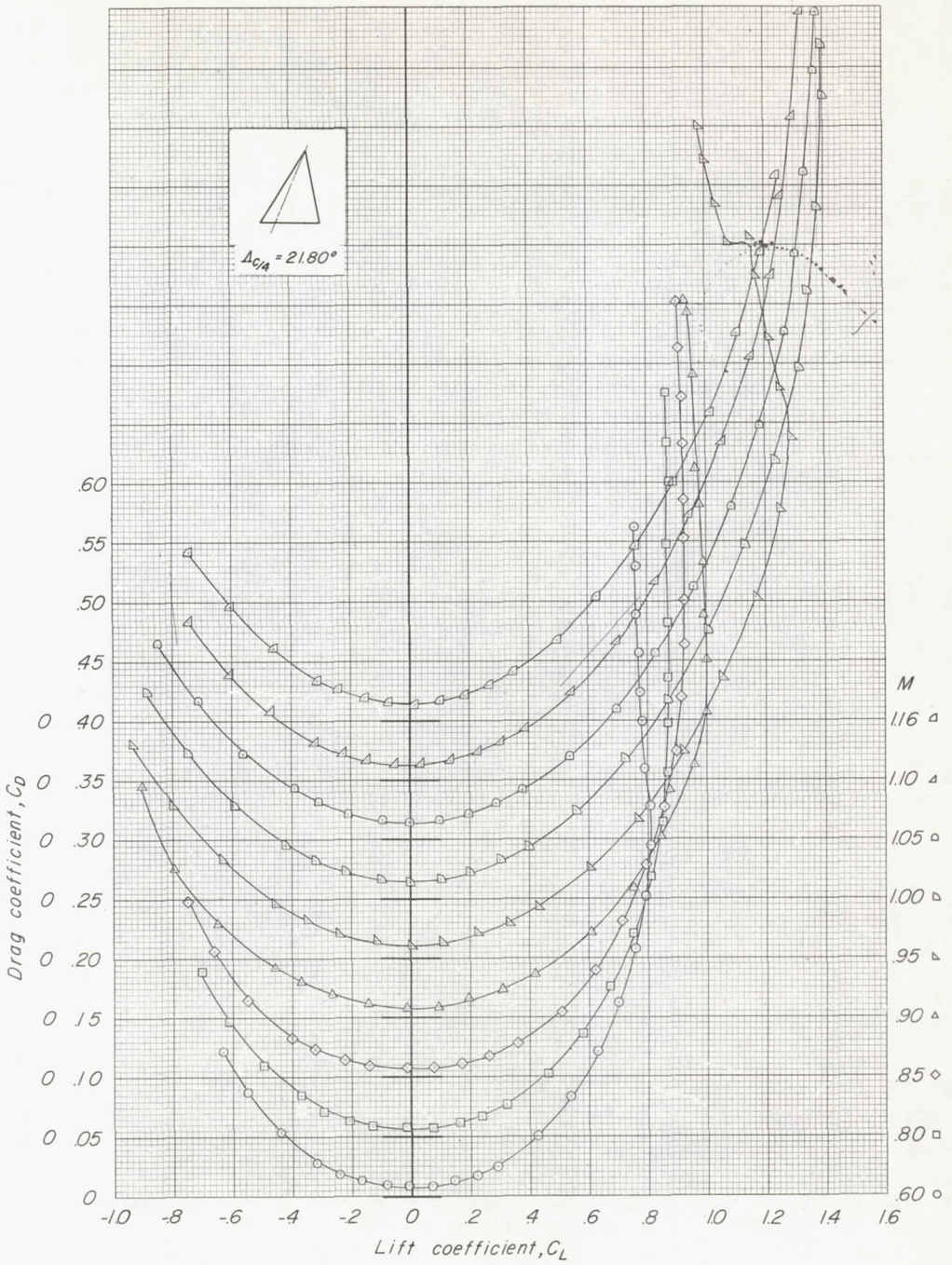
(b) A = 4.

Figure 7.- Continued.



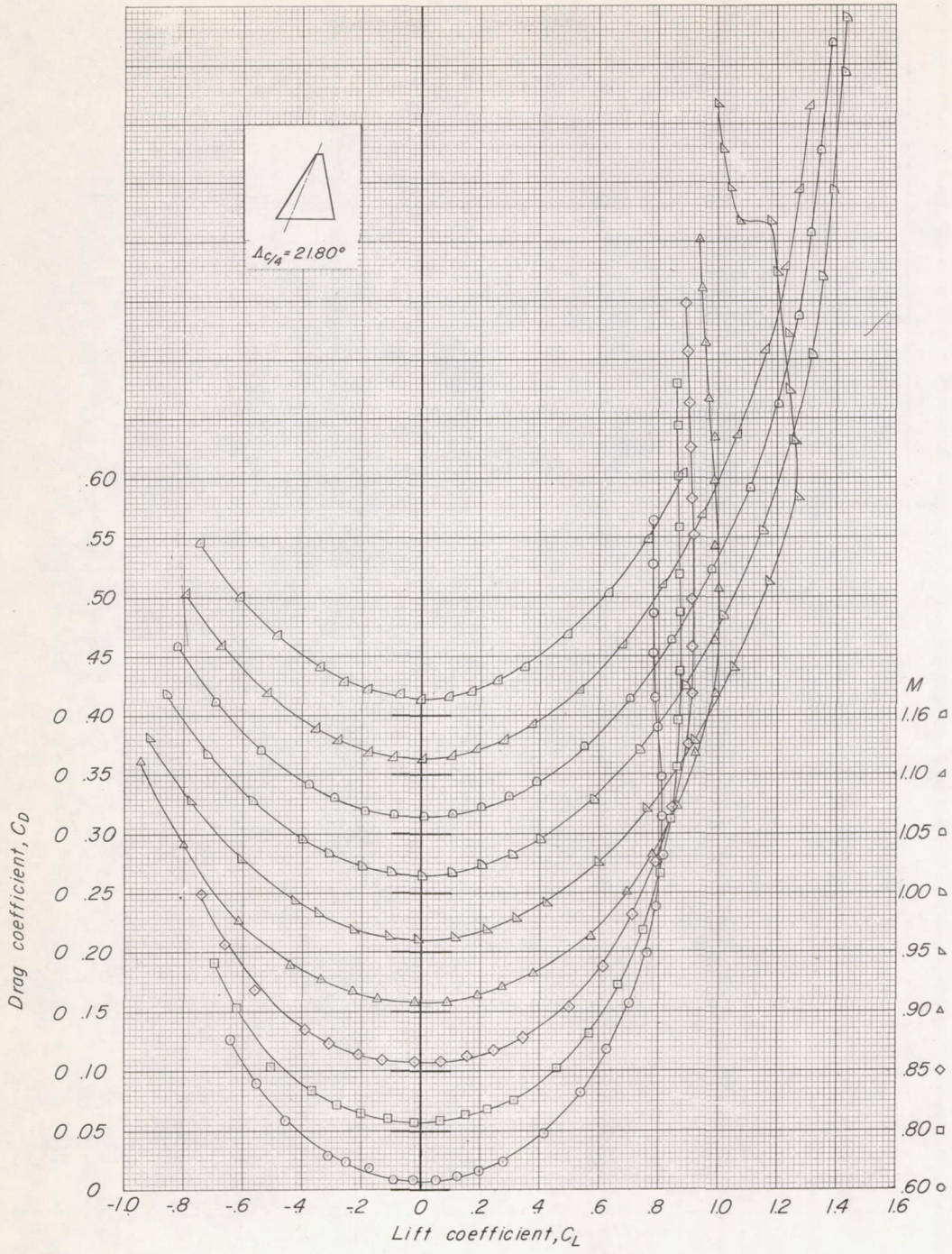
(c) A = 3.

Figure 7.- Concluded.



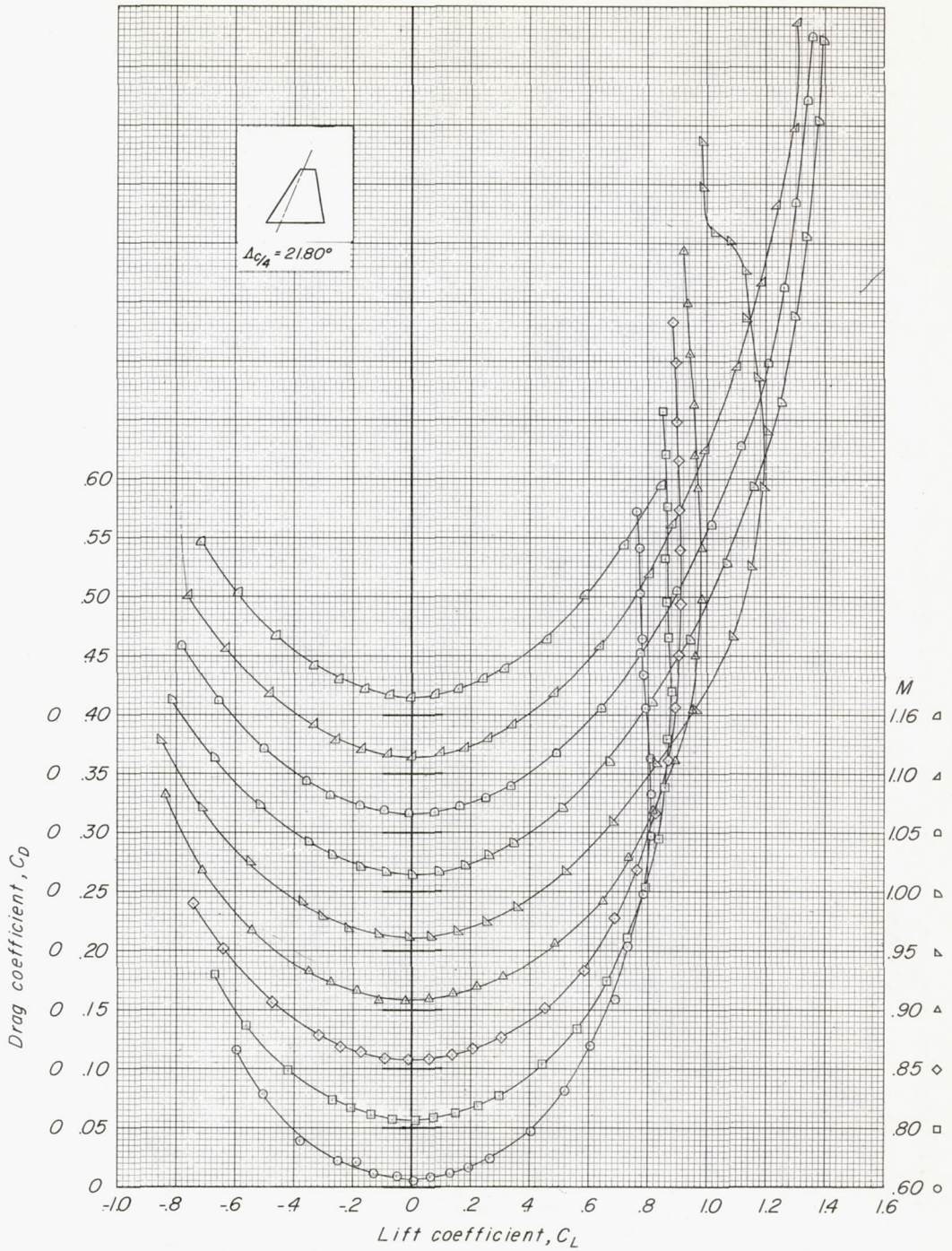
(a) A = 5.

Figure 8.- Variation of drag coefficient with lift coefficient; $\Lambda_c/4 = 21.80°$.



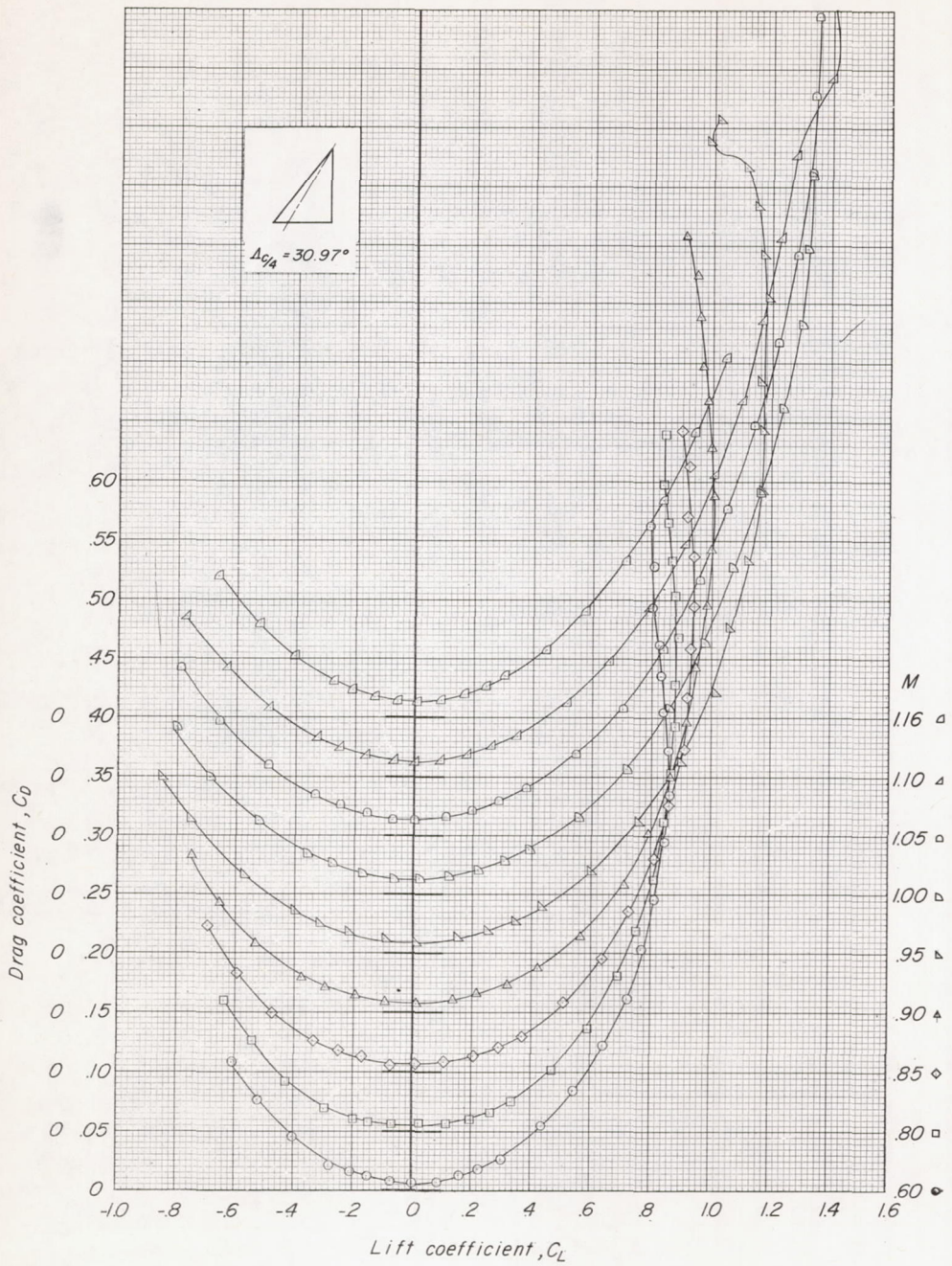
(b) A = 4.

Figure 8.- Continued.



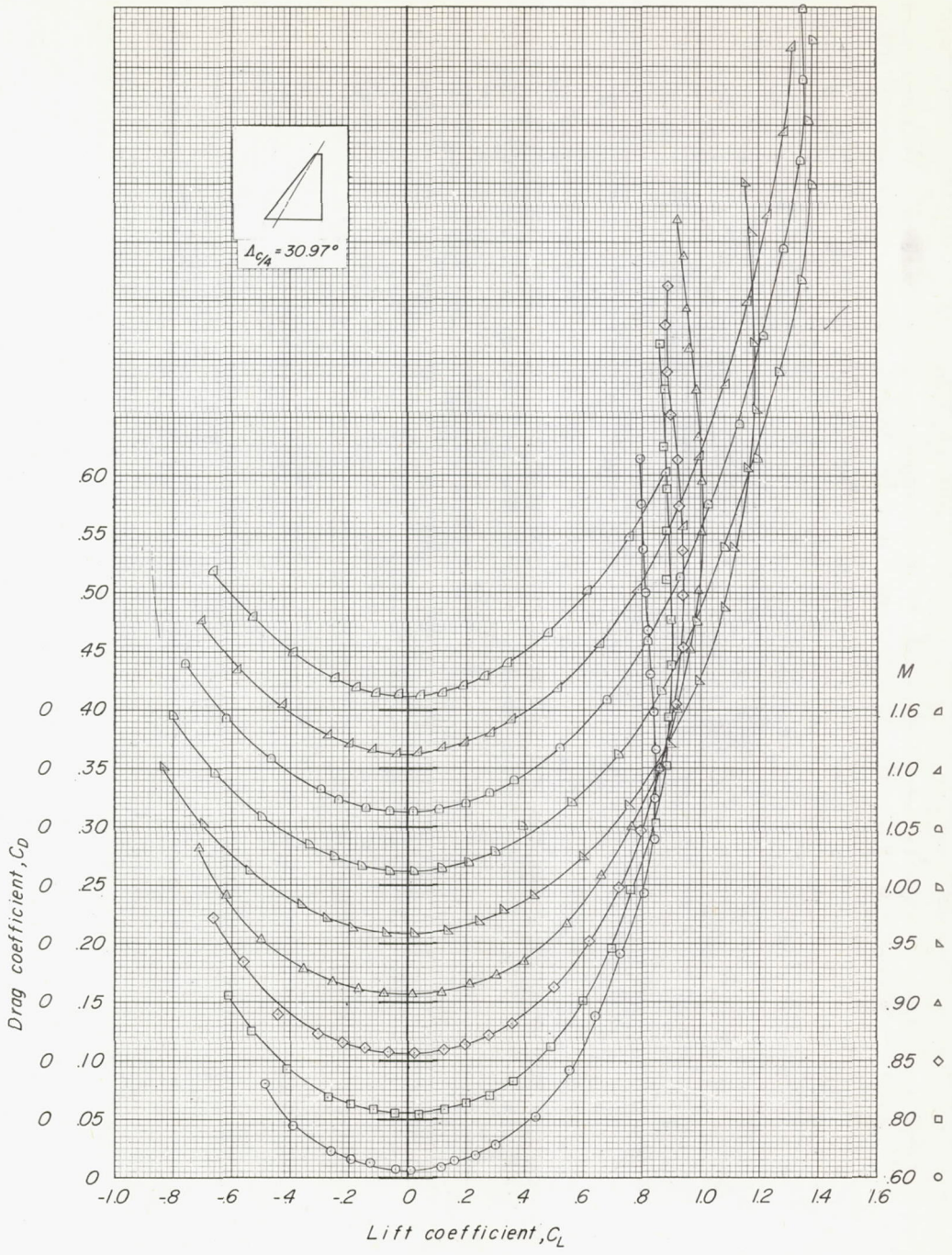
(c) A = 3.

Figure 8.- Concluded.



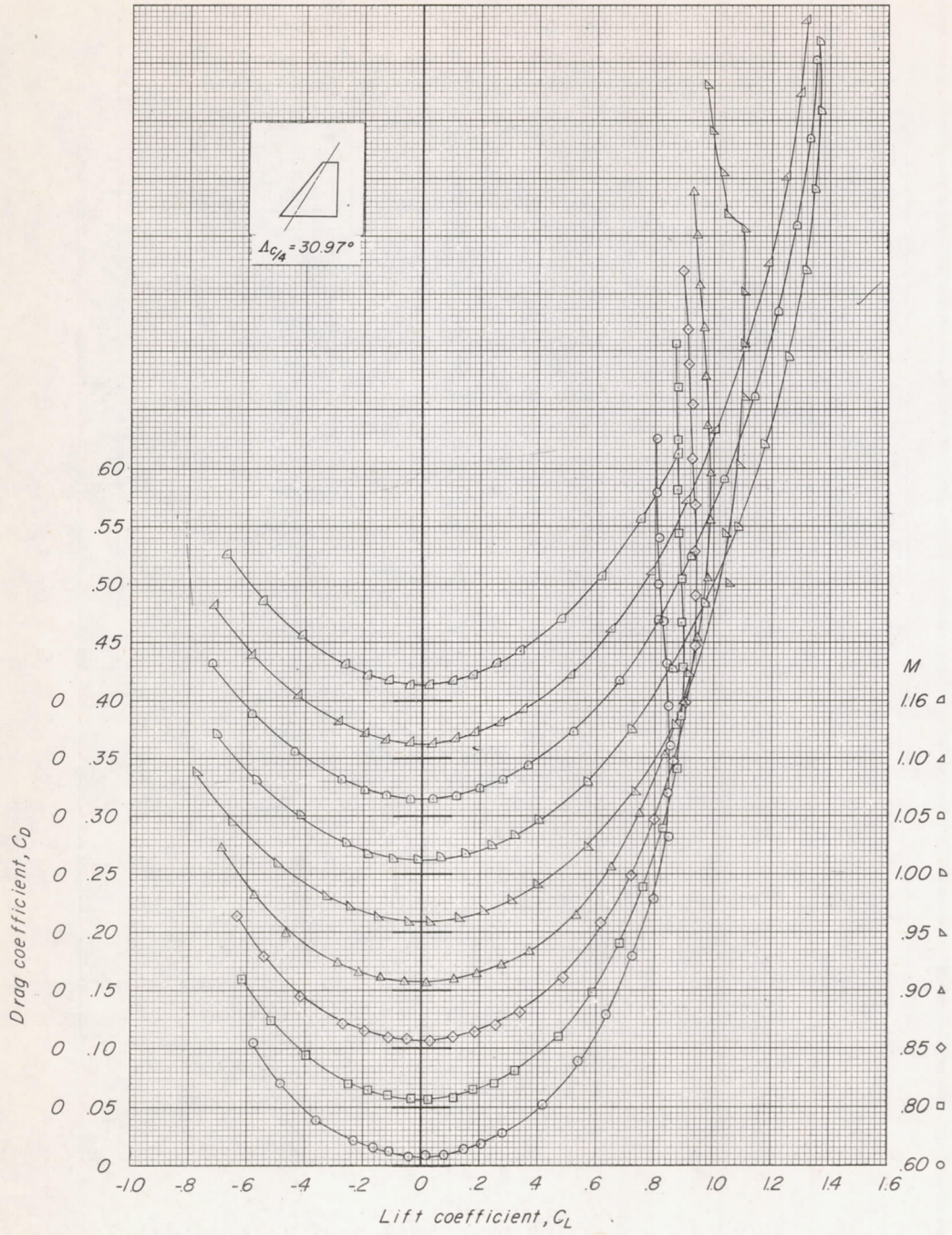
(a) A = 5.

Figure 9.- Variation of drag coefficient with lift coefficient; $\Lambda_{c/4} = 30.97^{\circ}$.



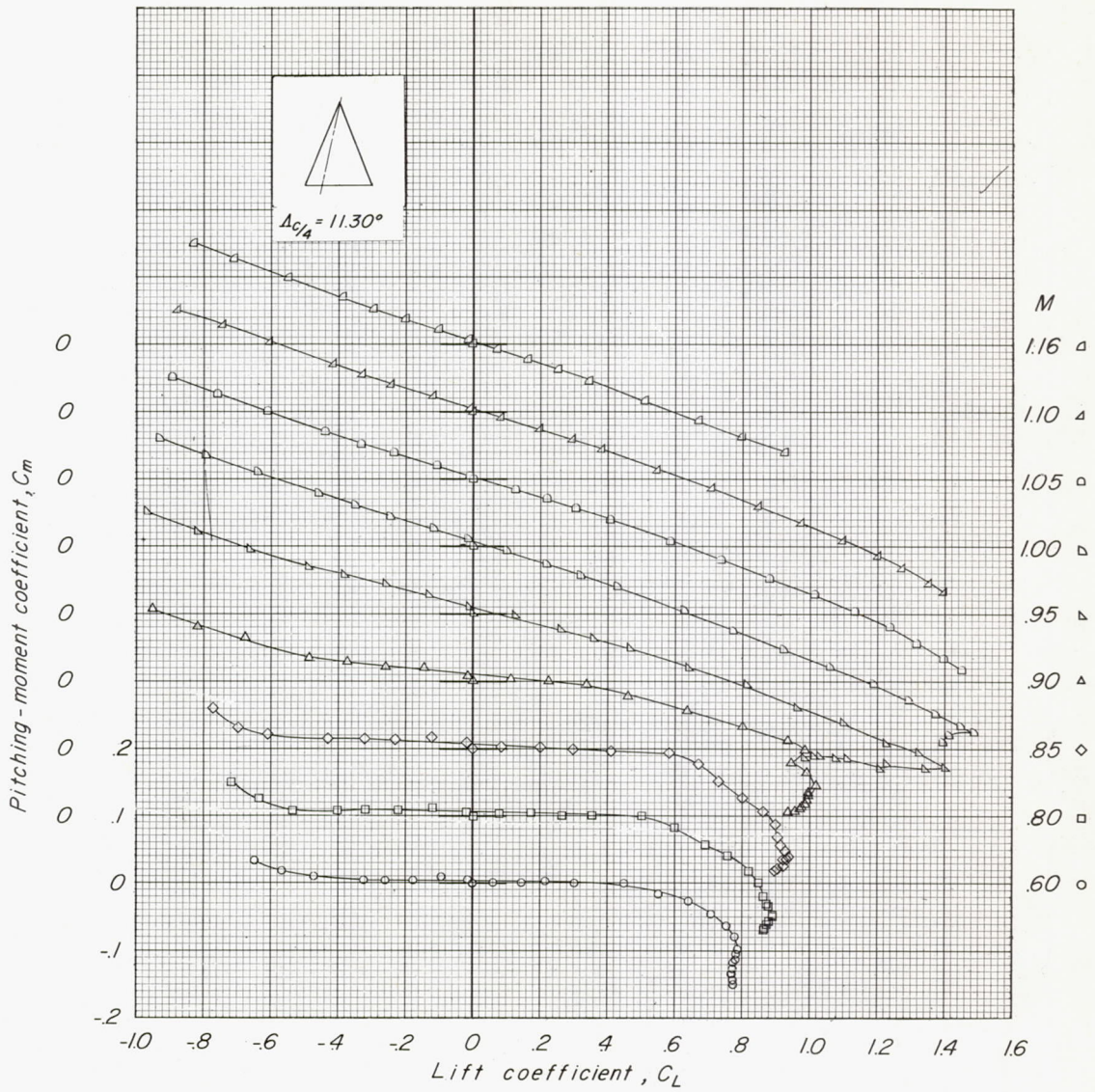
(b) A = 4.

Figure 9.- Continued.



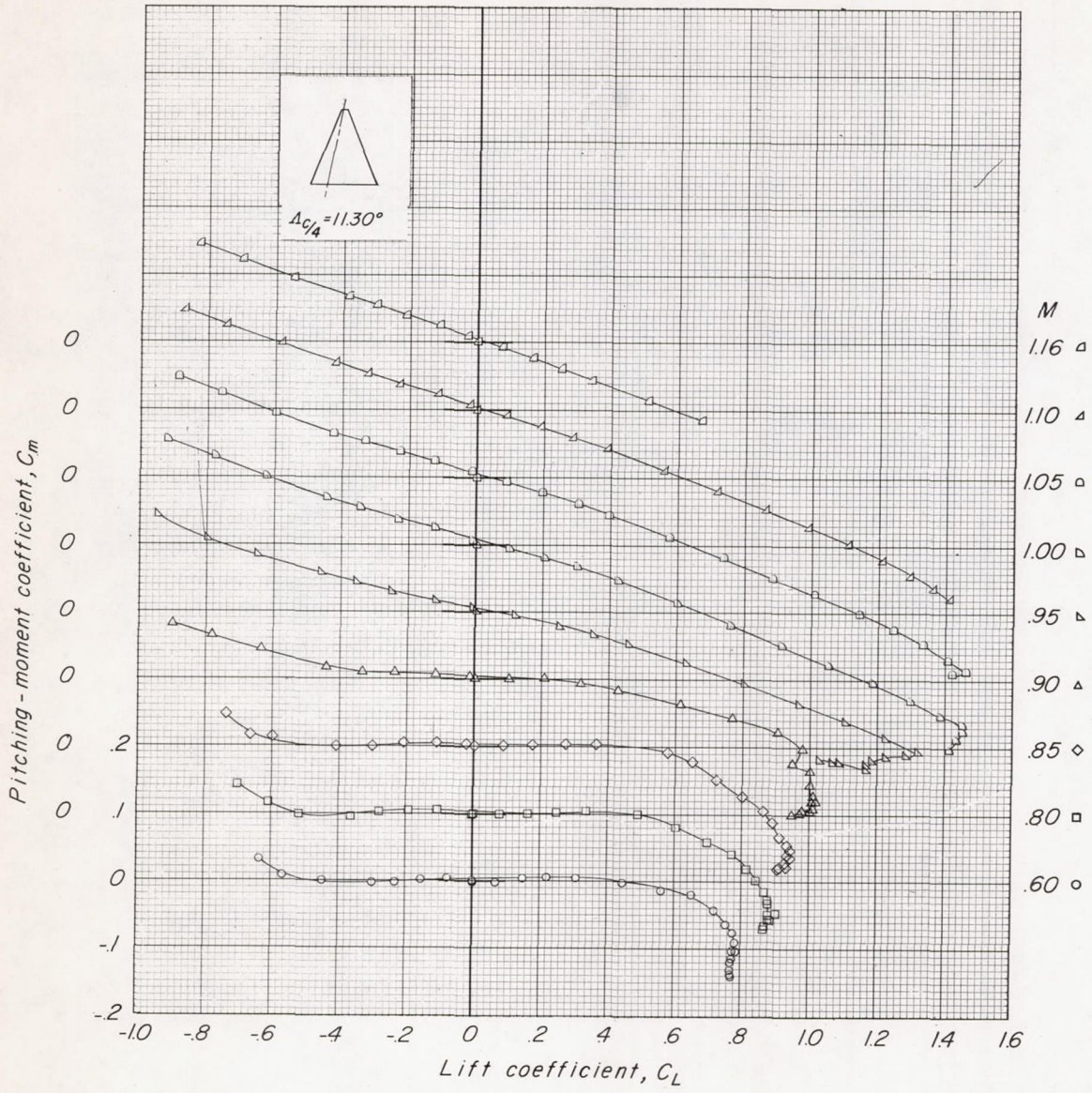
(c) A = 3.

Figure 9.- Concluded.



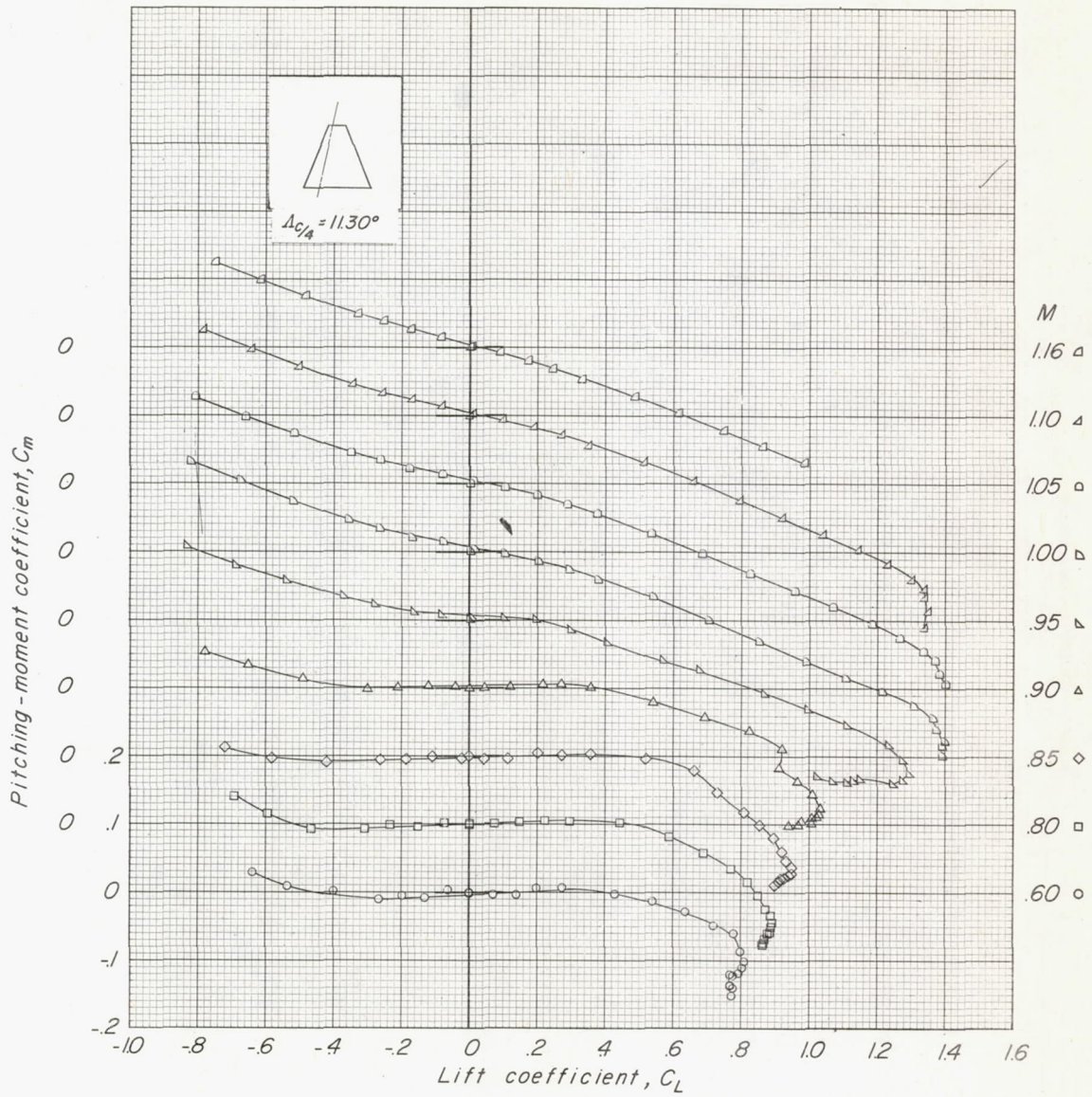
(a) A = 5.

Figure 10.- Variation of pitching-moment coefficient with lift coefficient; $\Lambda_{c/4} = 11.30^{\circ}$.



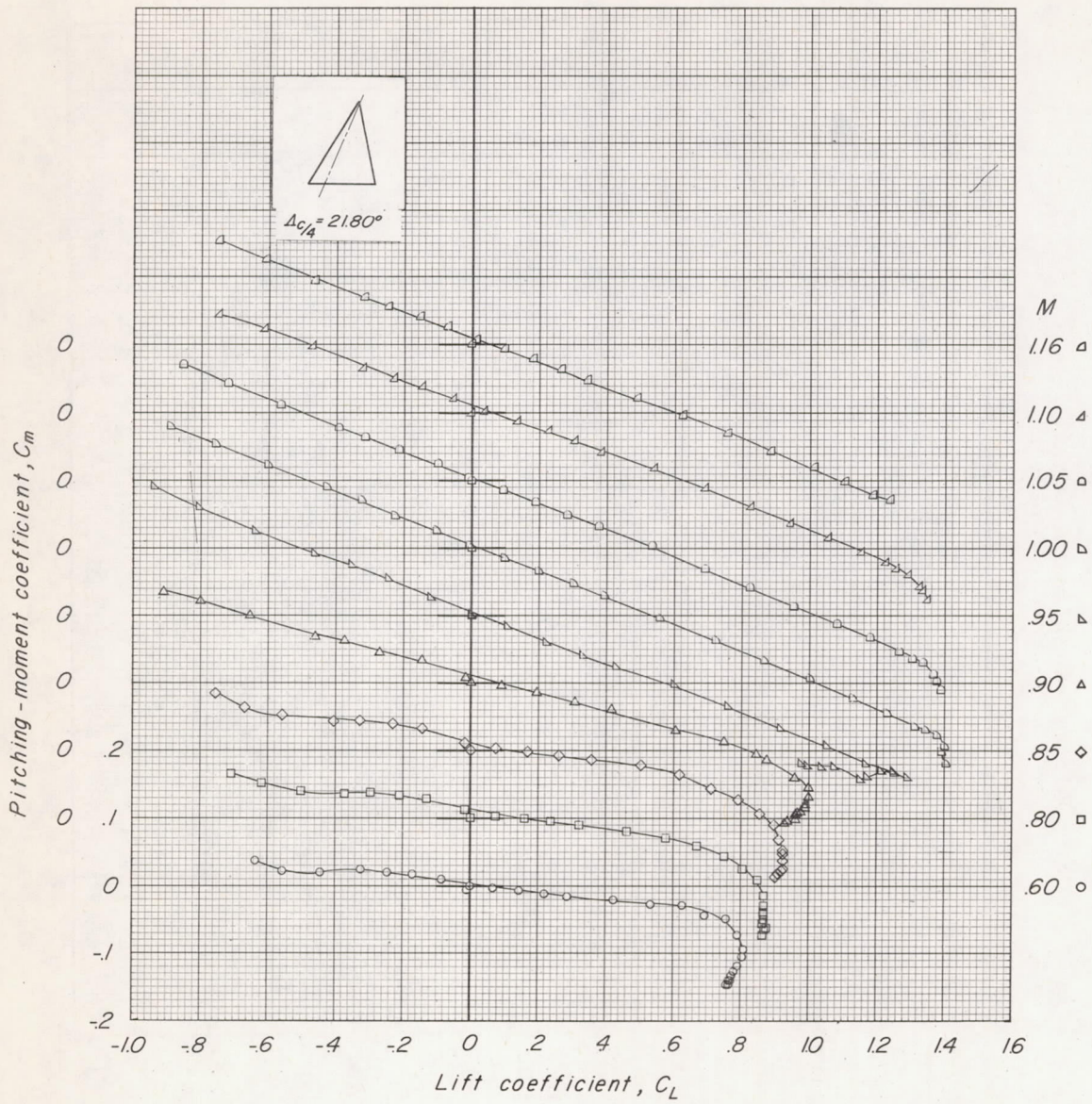
(b) A = 4.

Figure 10.- Continued.



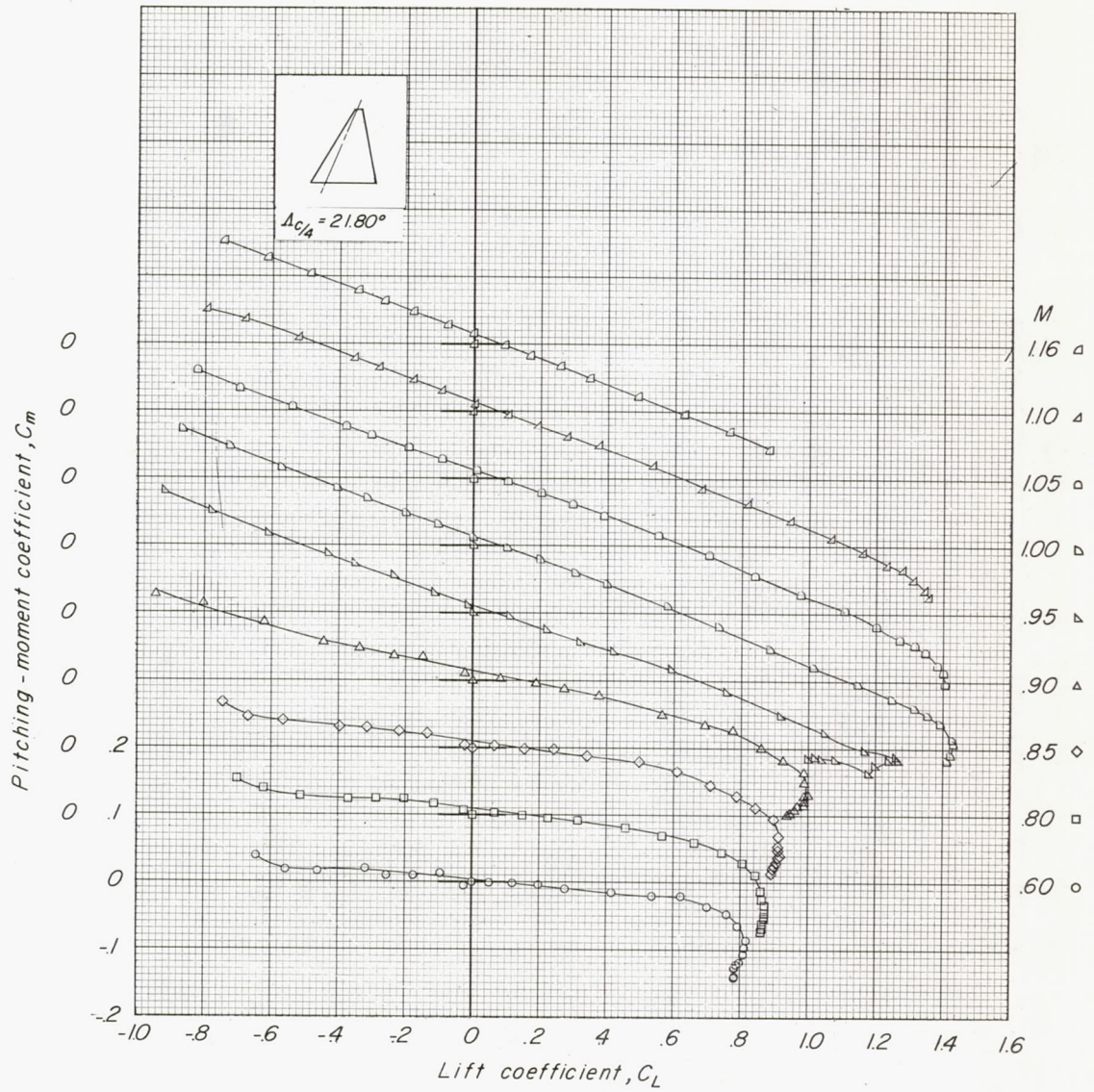
(c) A = 3.

Figure 10.- Concluded.



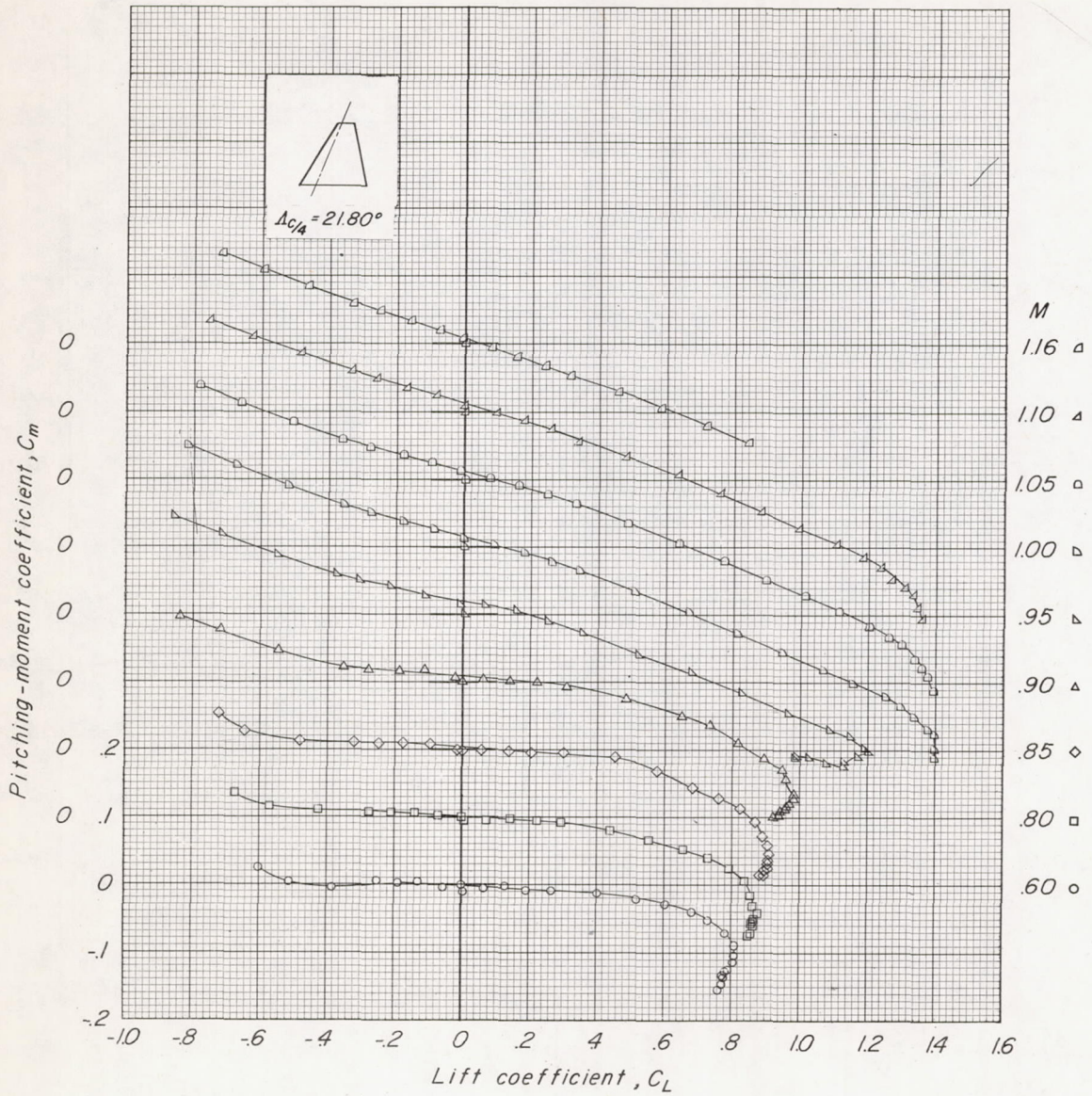
(a) A = 5.

Figure 11.- Variation of pitching-moment coefficient with lift coefficient; $\Lambda_{c/4}$ = 21.80°.



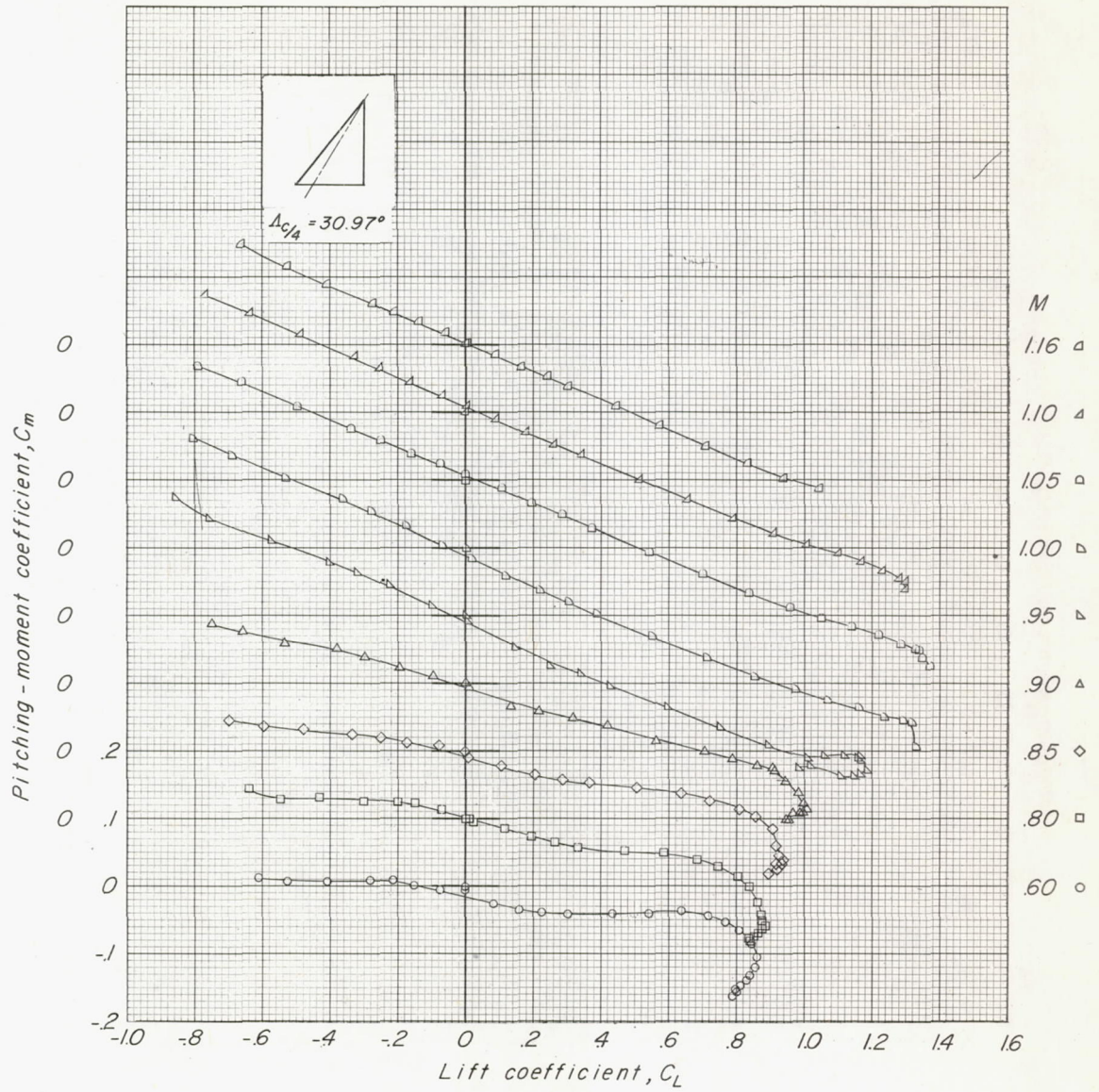
(b) A = 4.

Figure 11.- Continued.



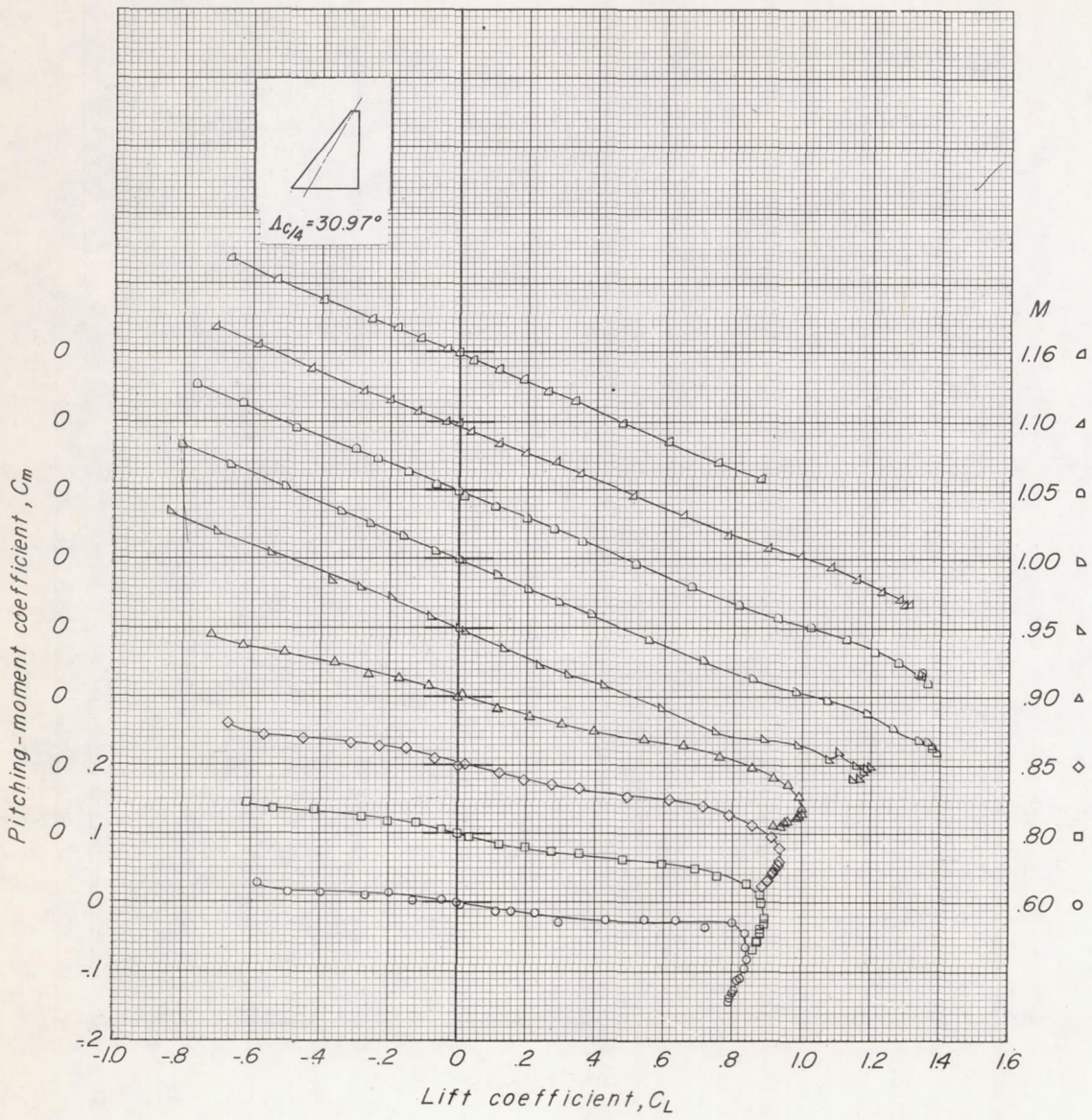
(c) A = 3.

Figure 11.- Concluded.



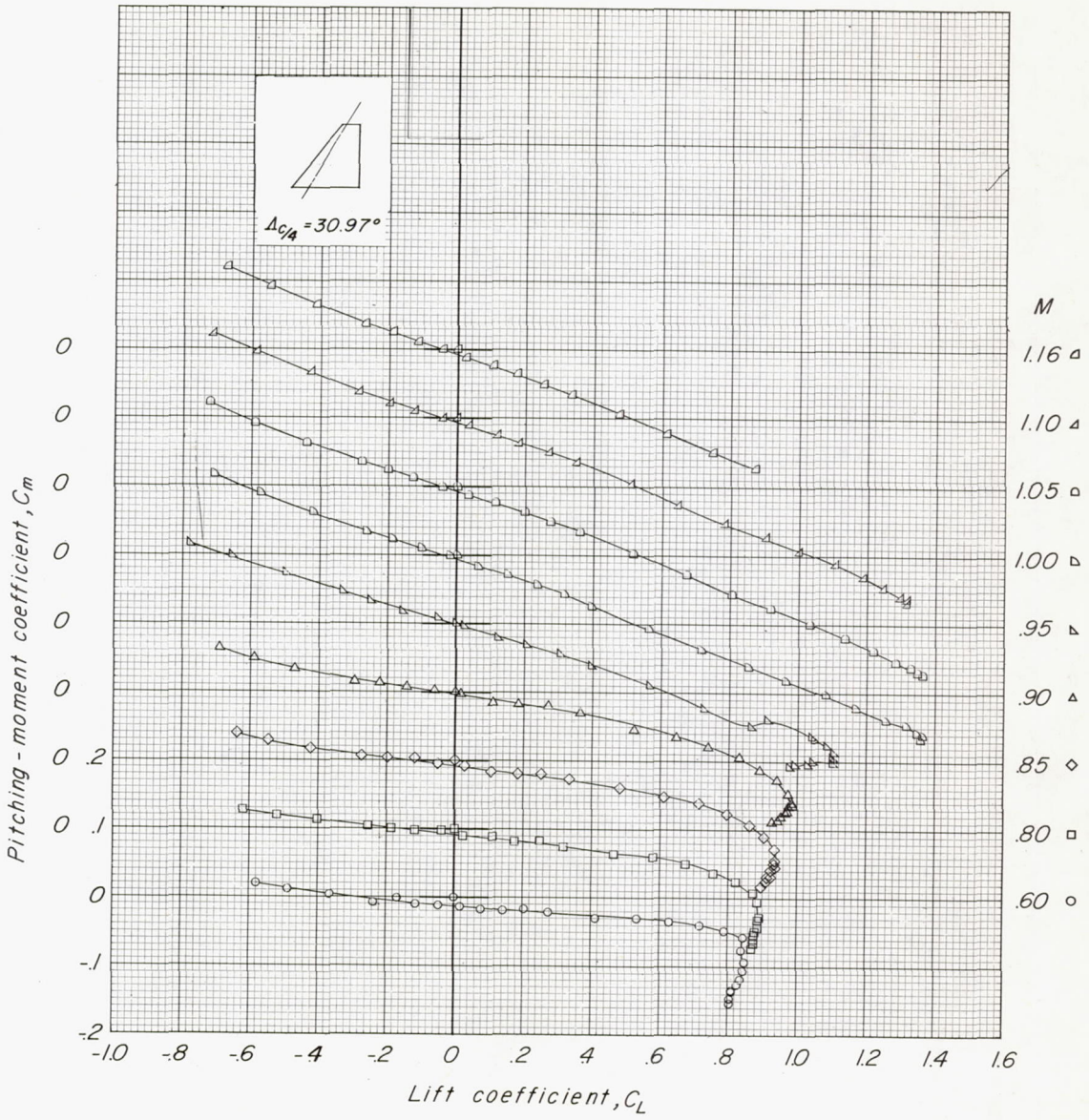
(a) A = 5.

Figure 12.- Variation of pitching-moment coefficient with lift coefficient; $\Lambda_{c/4} = 30.97°$.



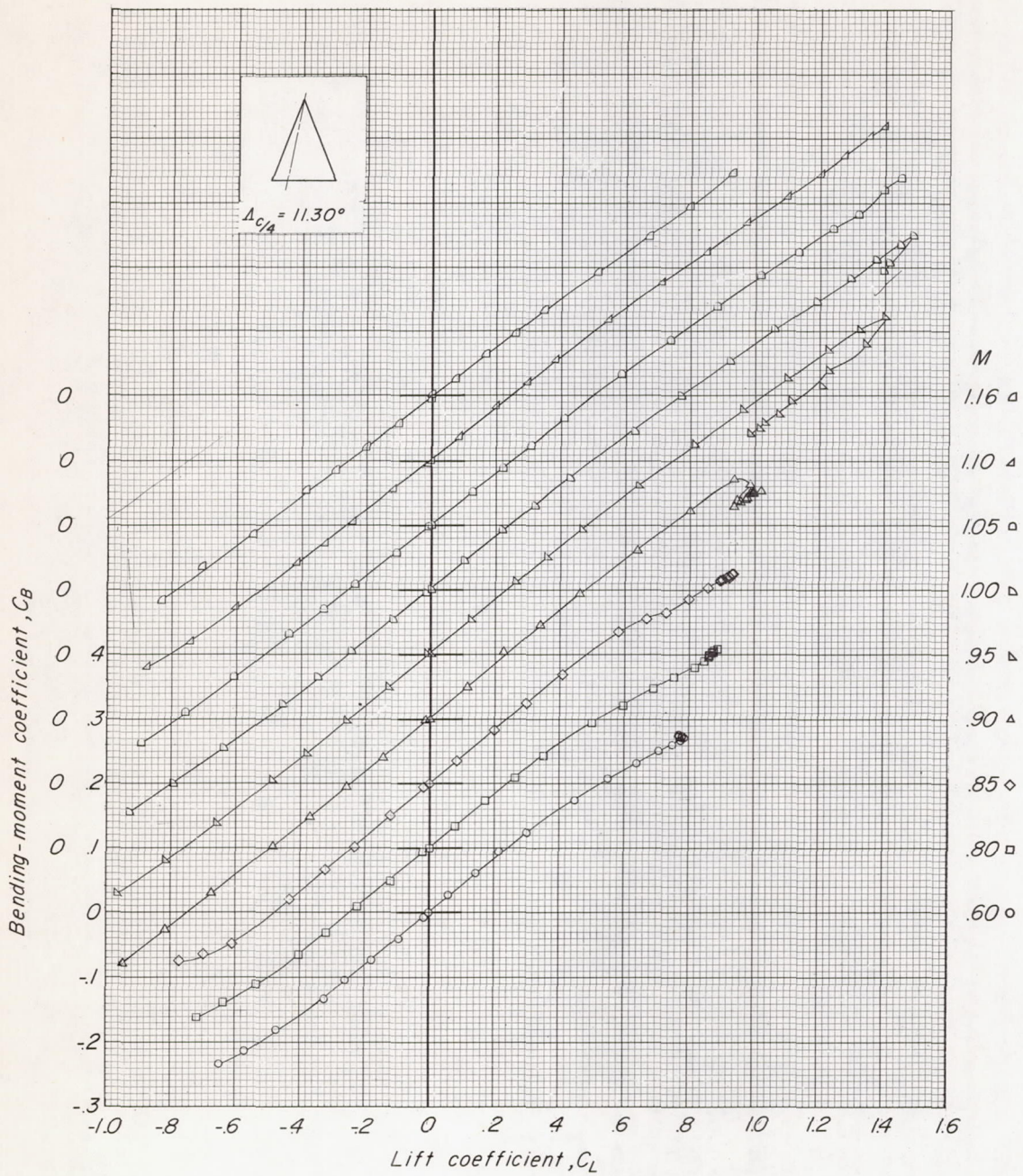
(b) A = 4.

Figure 12.- Continued.



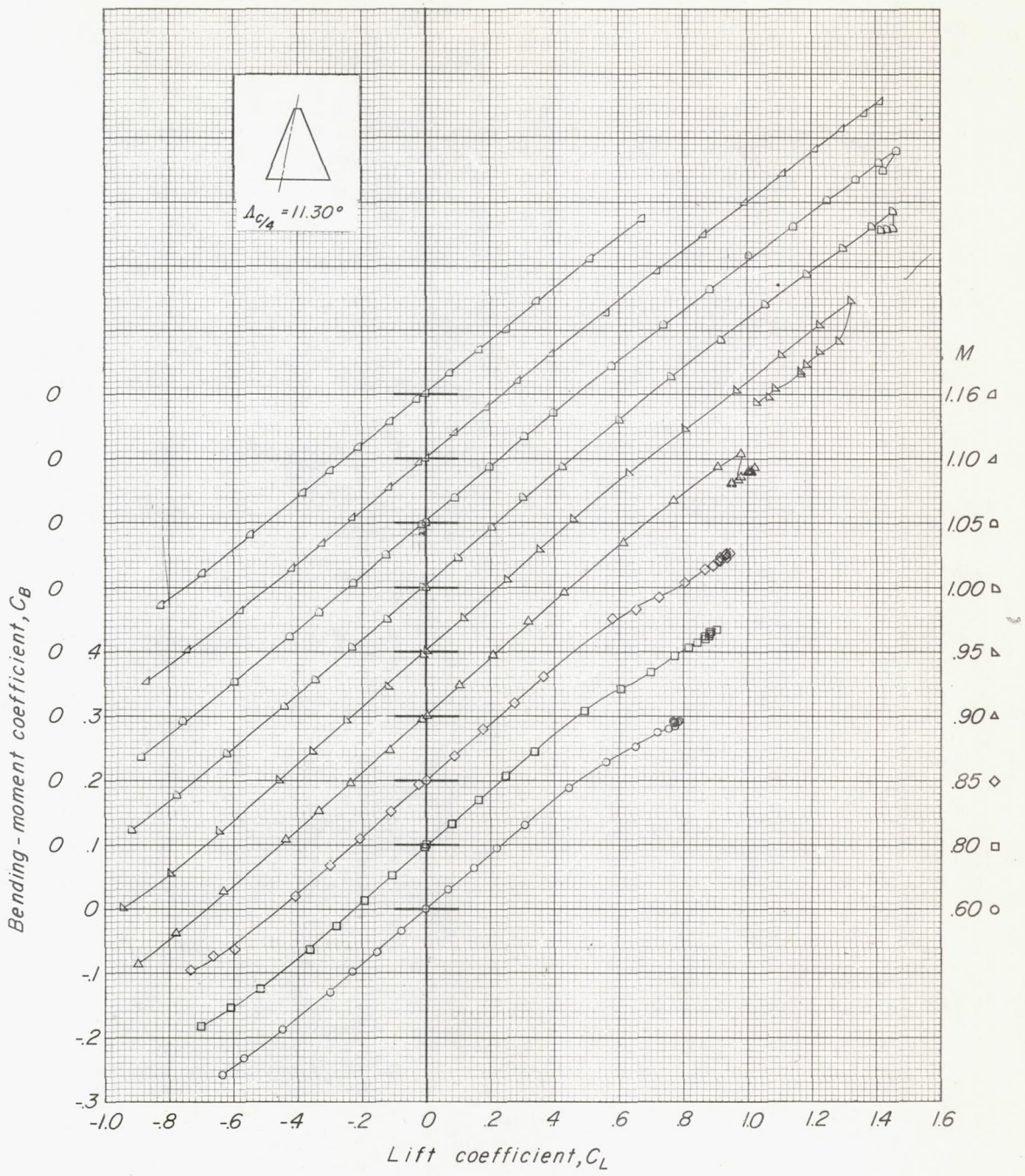
(c) A = 3.

Figure 12.- Concluded.



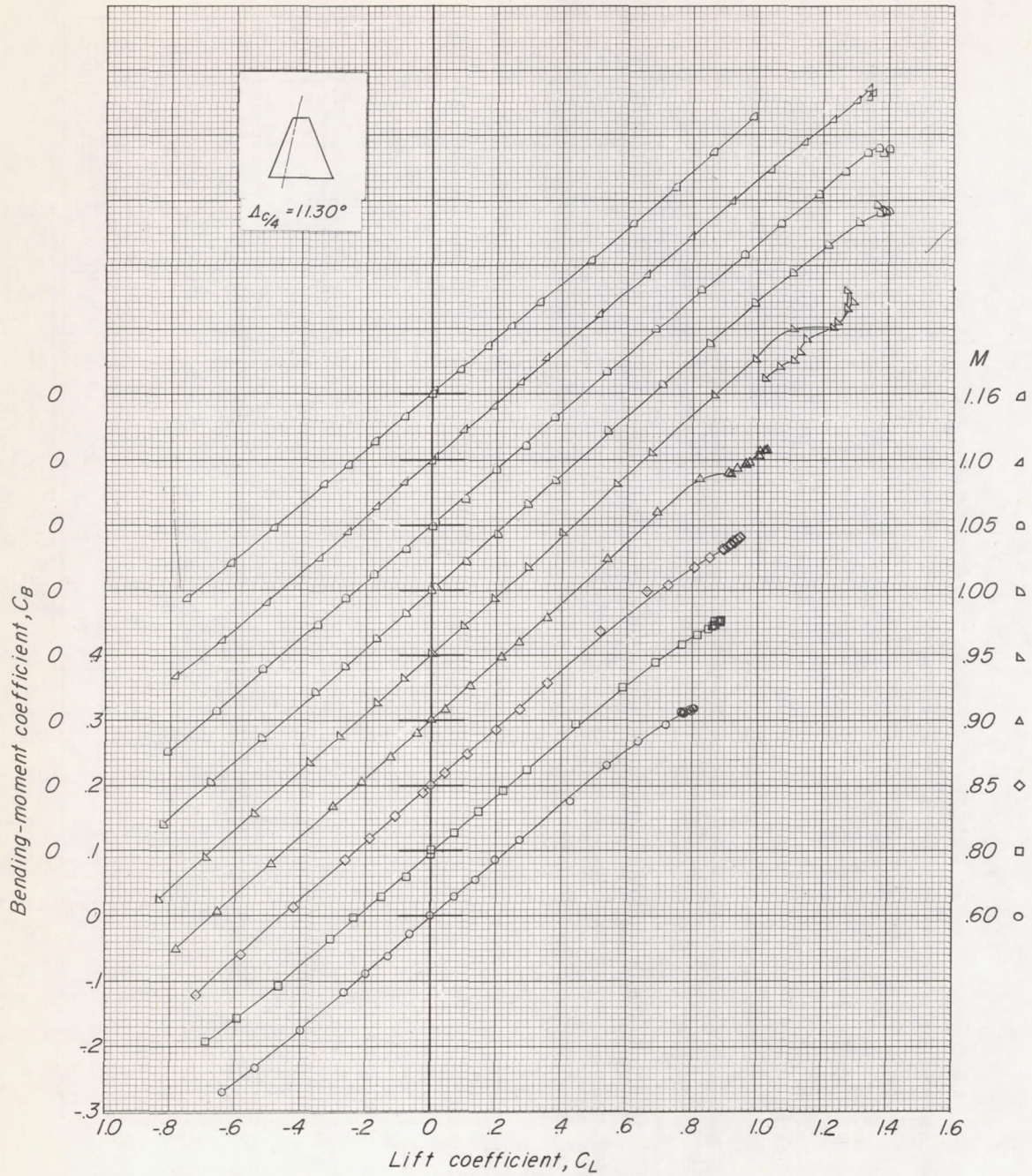
(a) A = 5.

Figure 13.- Variation of bending-moment coefficient with lift coefficient; $\Lambda_{c/4}$ = 11.30°.



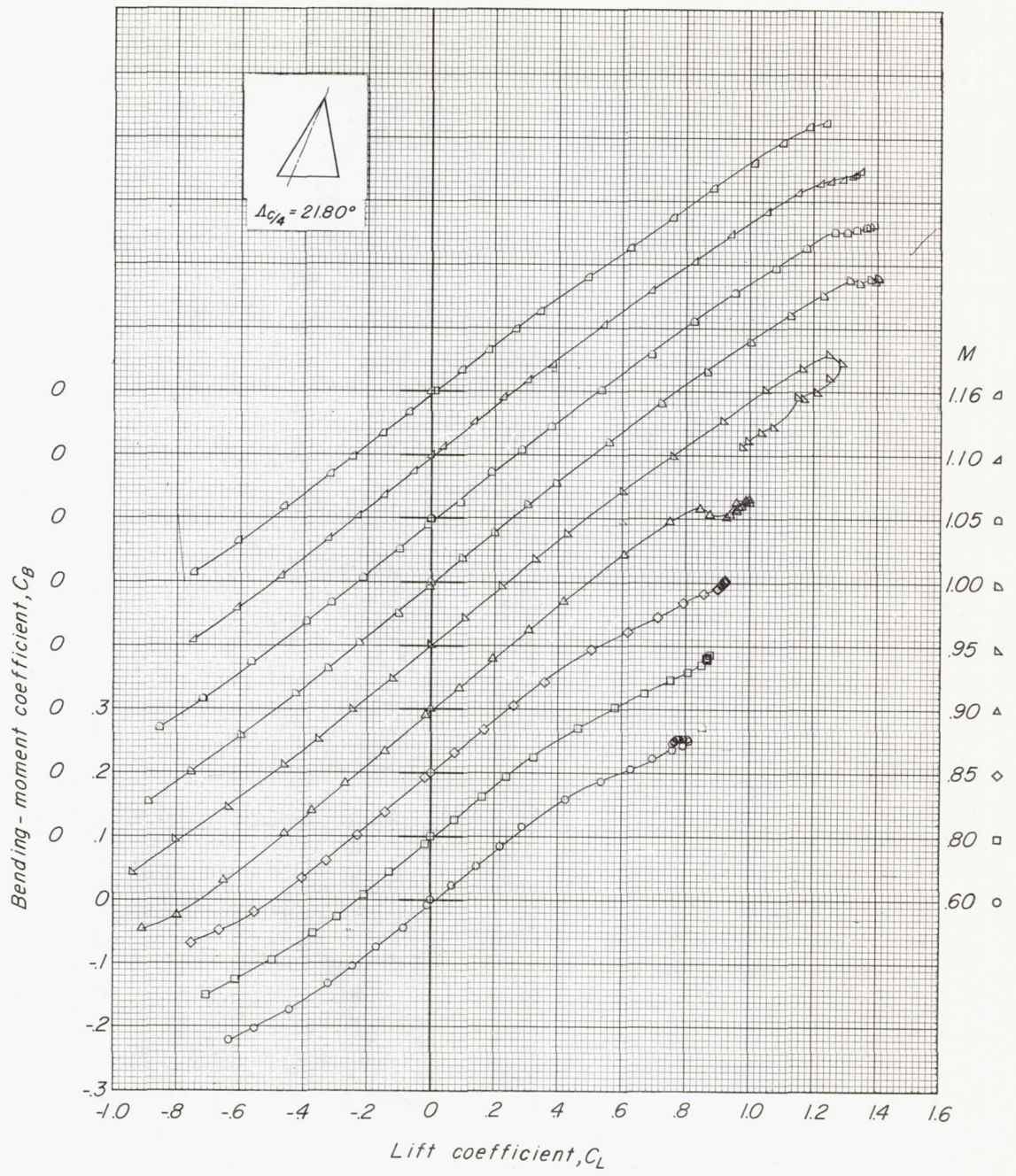
(b) A = 4.

Figure 13.- Continued.



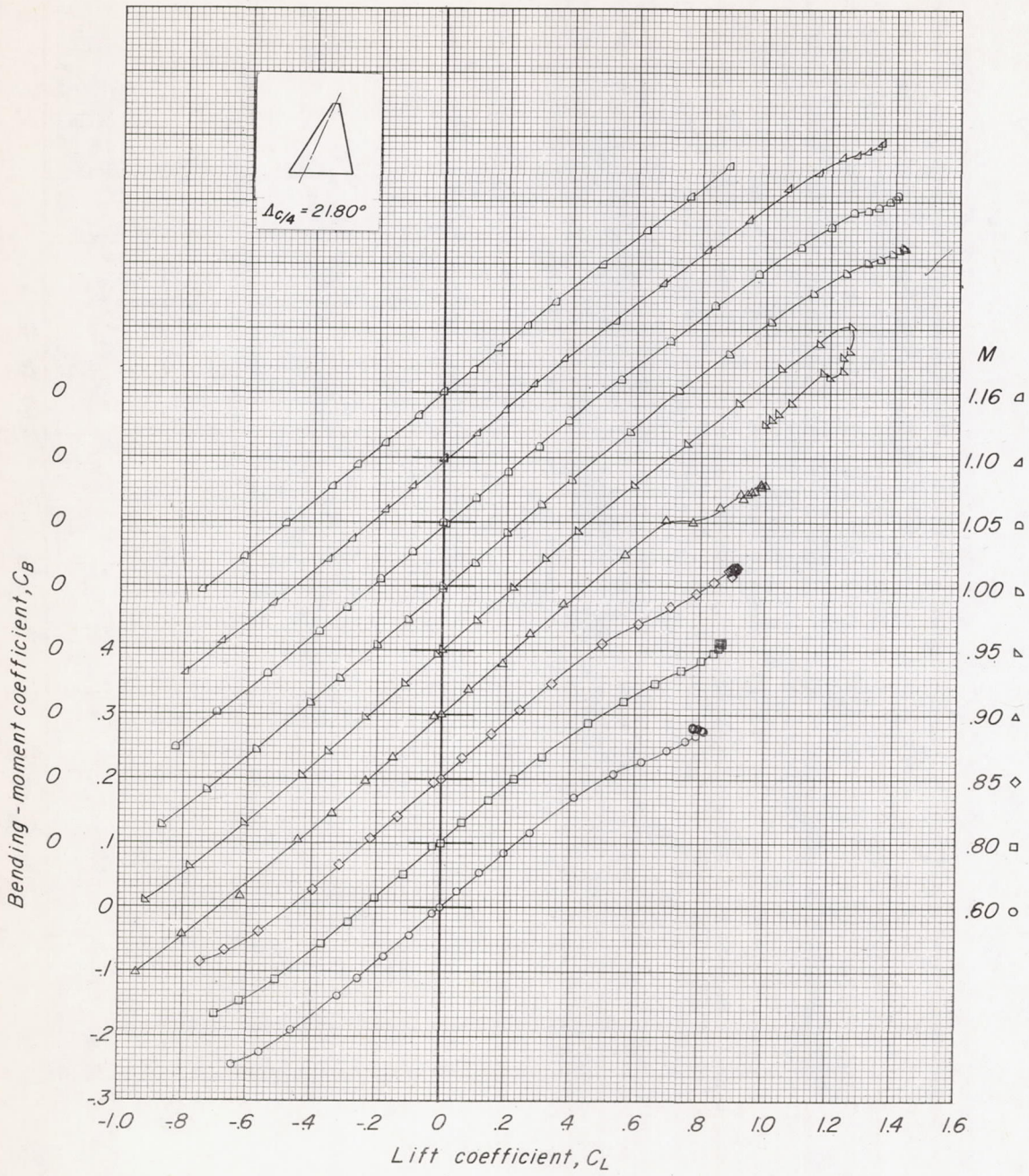
(c) A = 3.

Figure 13.- Concluded.



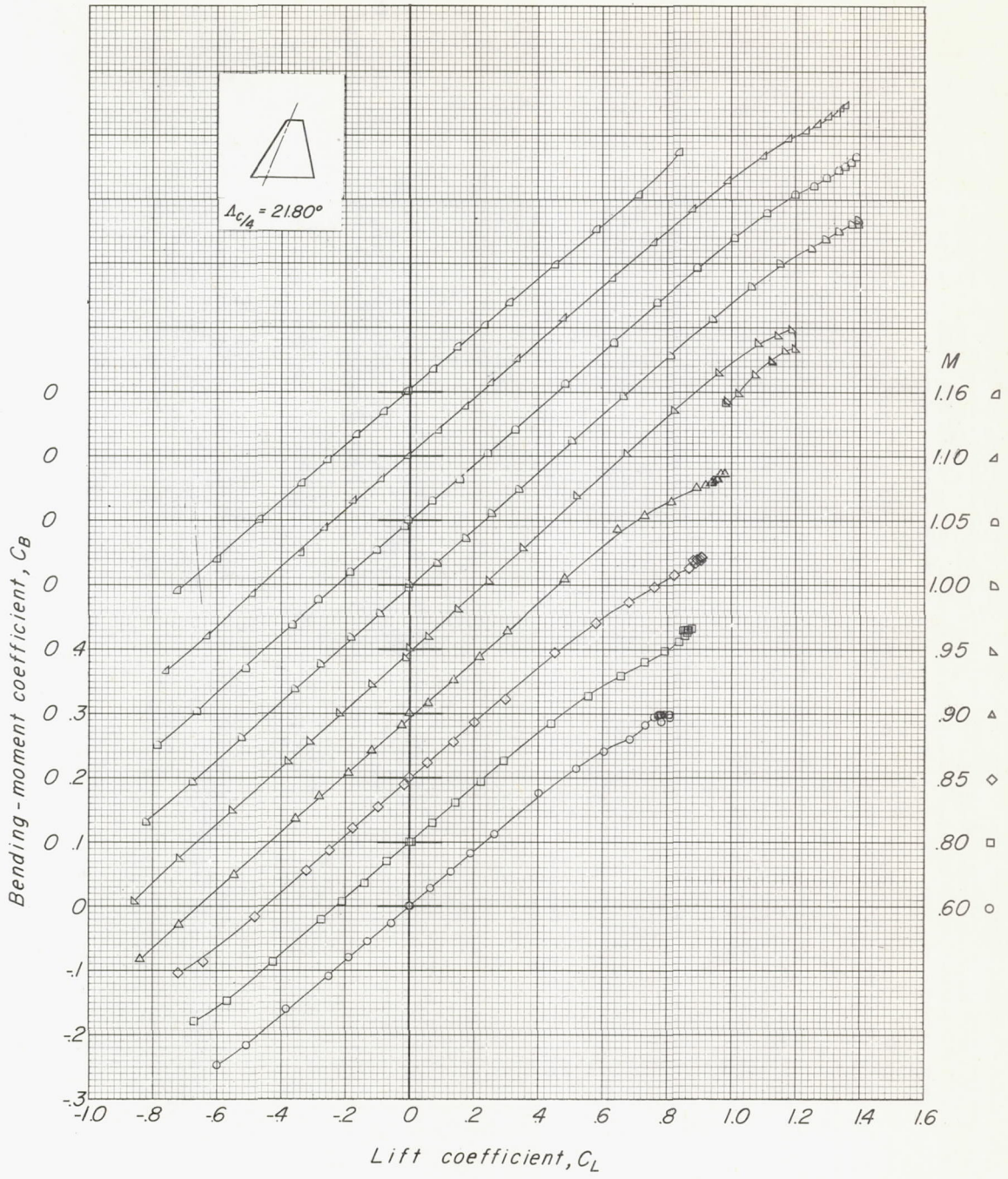
(a) A = 5.

Figure 14.- Variation of bending-moment coefficient with lift coefficient; $\Lambda_{c/4} = 21.80°$.



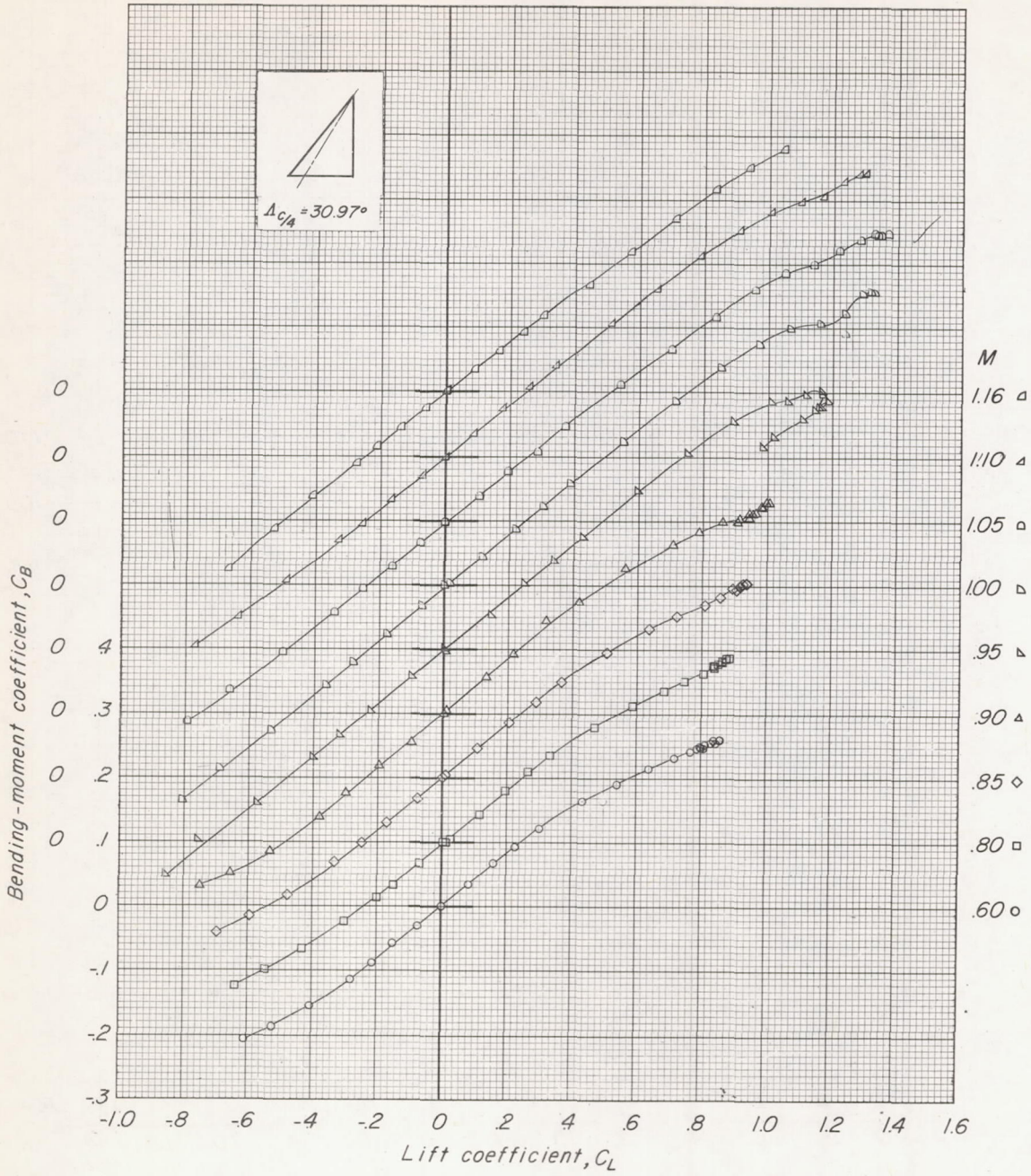
(b) A = 4.

Figure 14.- Continued.



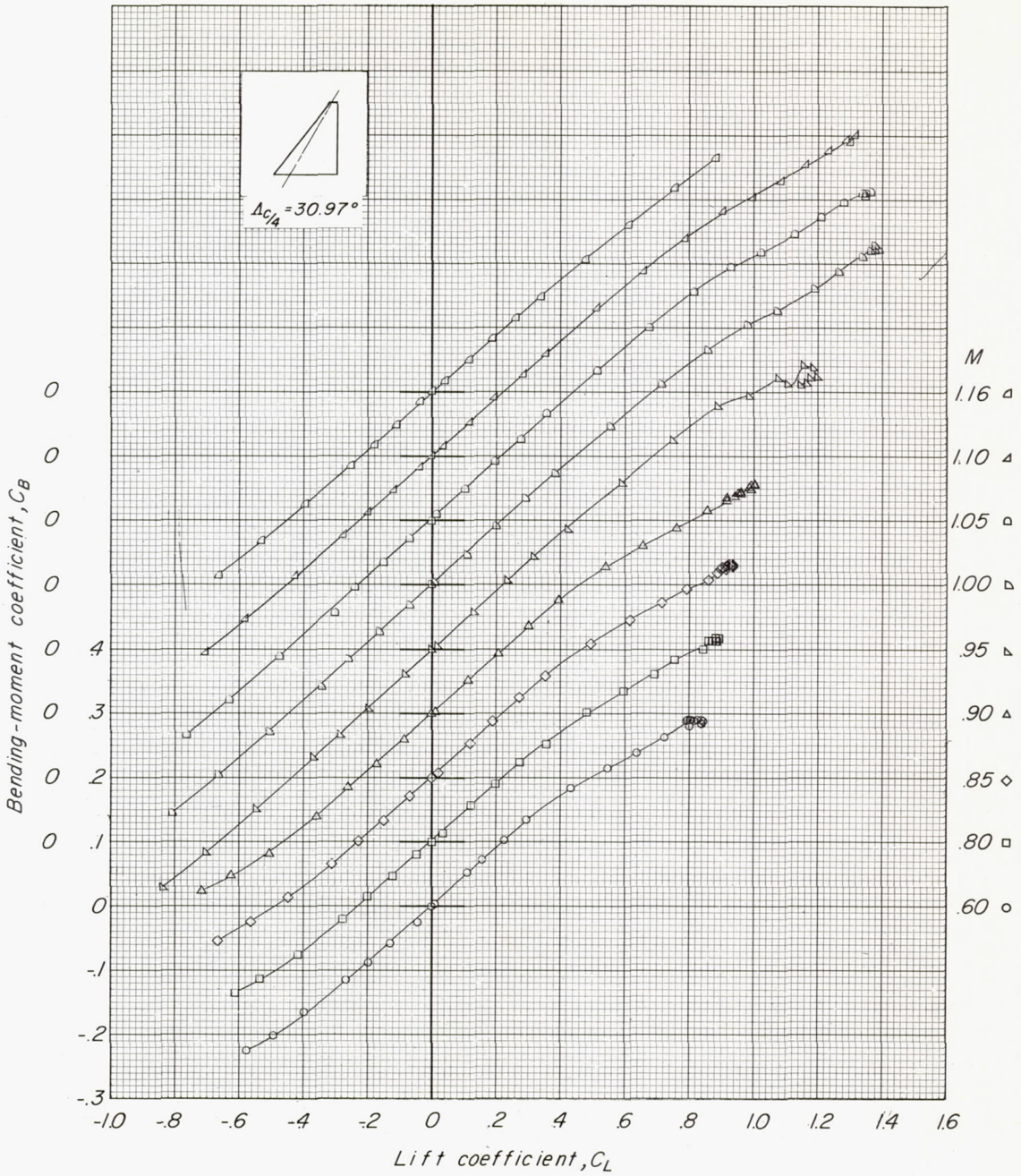
(c) A = 3.

Figure 14.- Concluded.



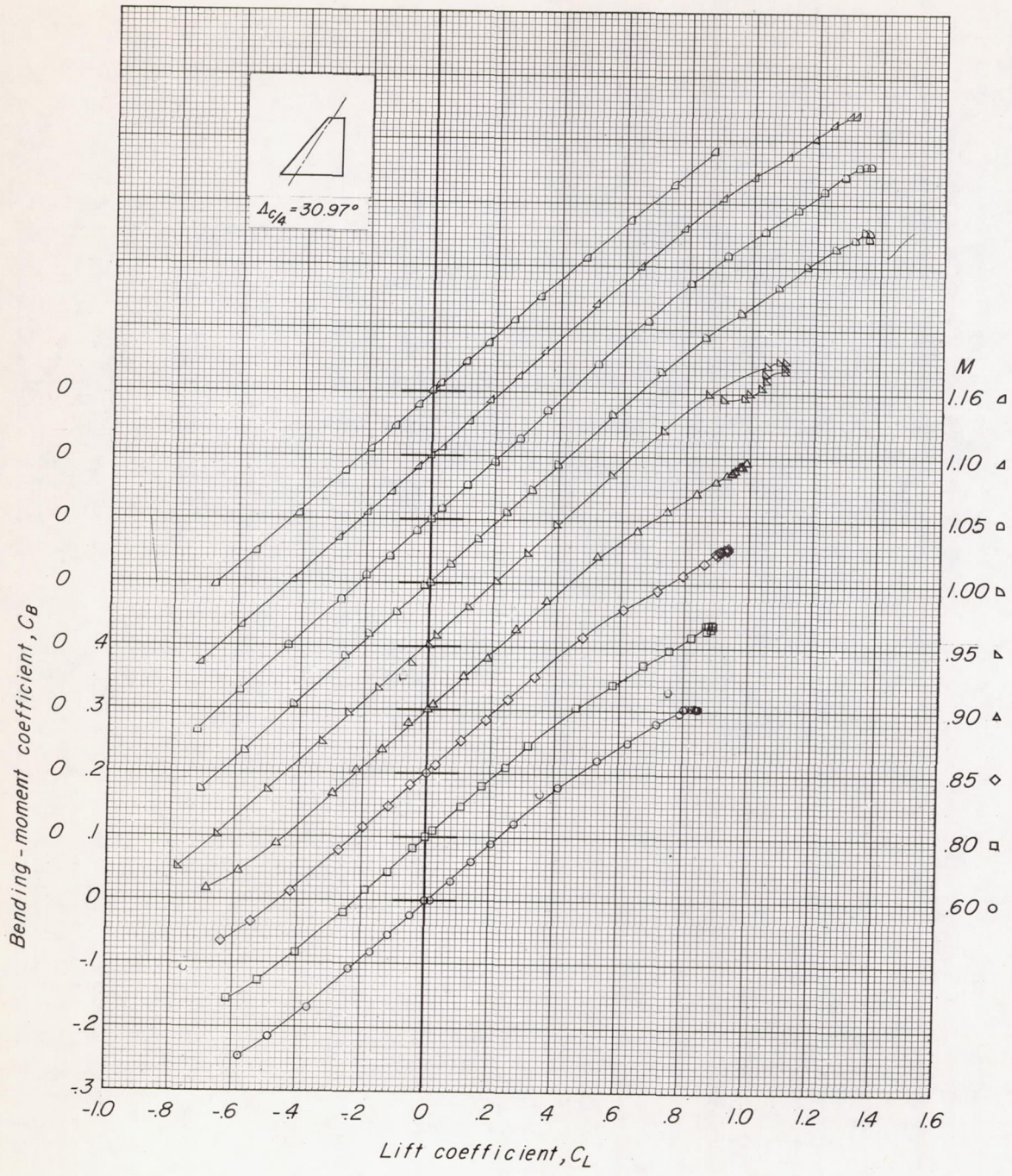
(a) A = 5.

Figure 15.- Variation of bending-moment coefficient with lift coefficient; $\Lambda_{c/4} = 30.97°$.



(b) A = 4.

Figure 15.- Continued.



(c) A = 3.

Figure 15.- Concluded.

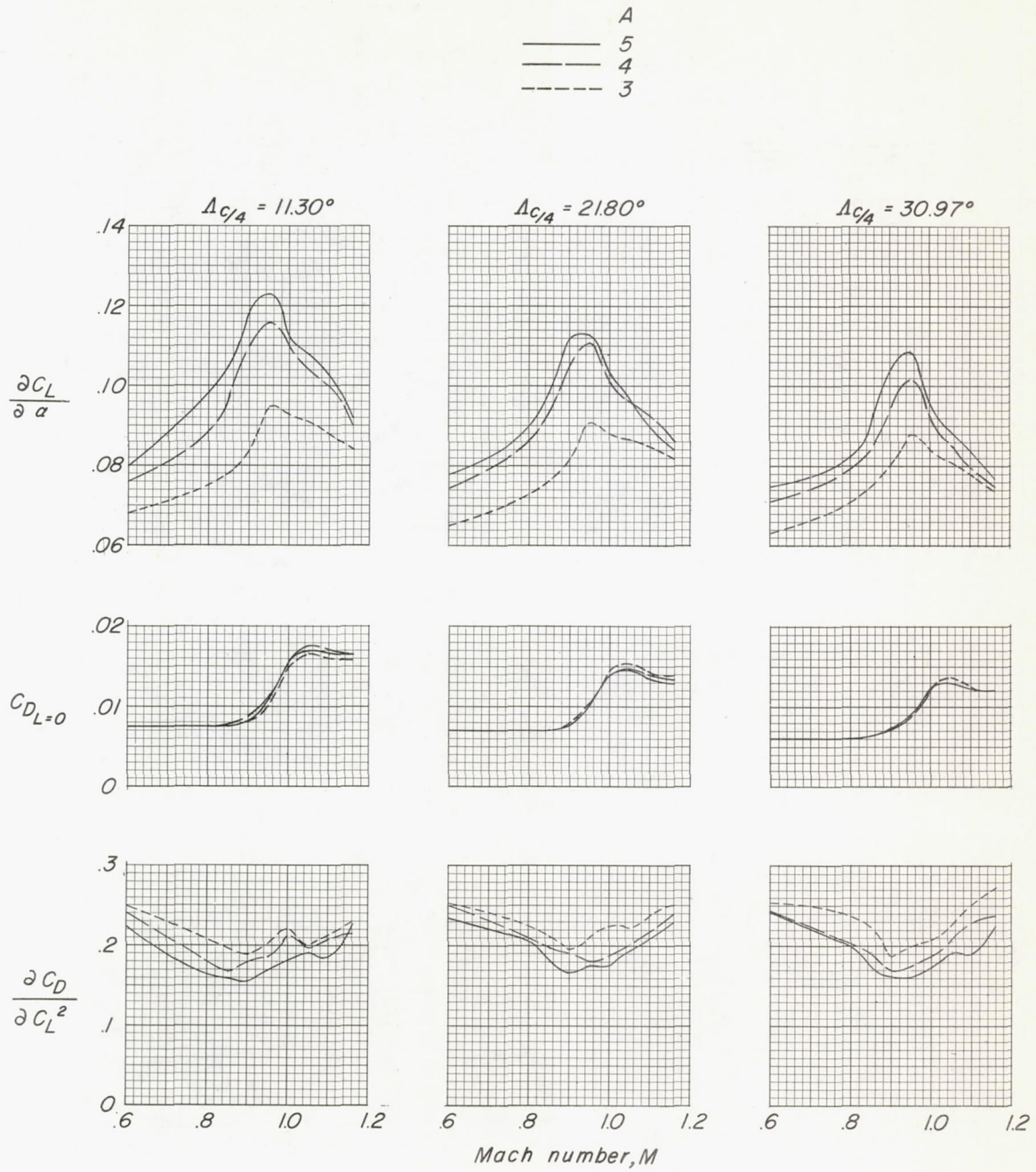


Figure 16.- Effect of aspect ratio and sweep on the variation of lift-curve slope, minimum drag, and drag due to lift with Mach number.

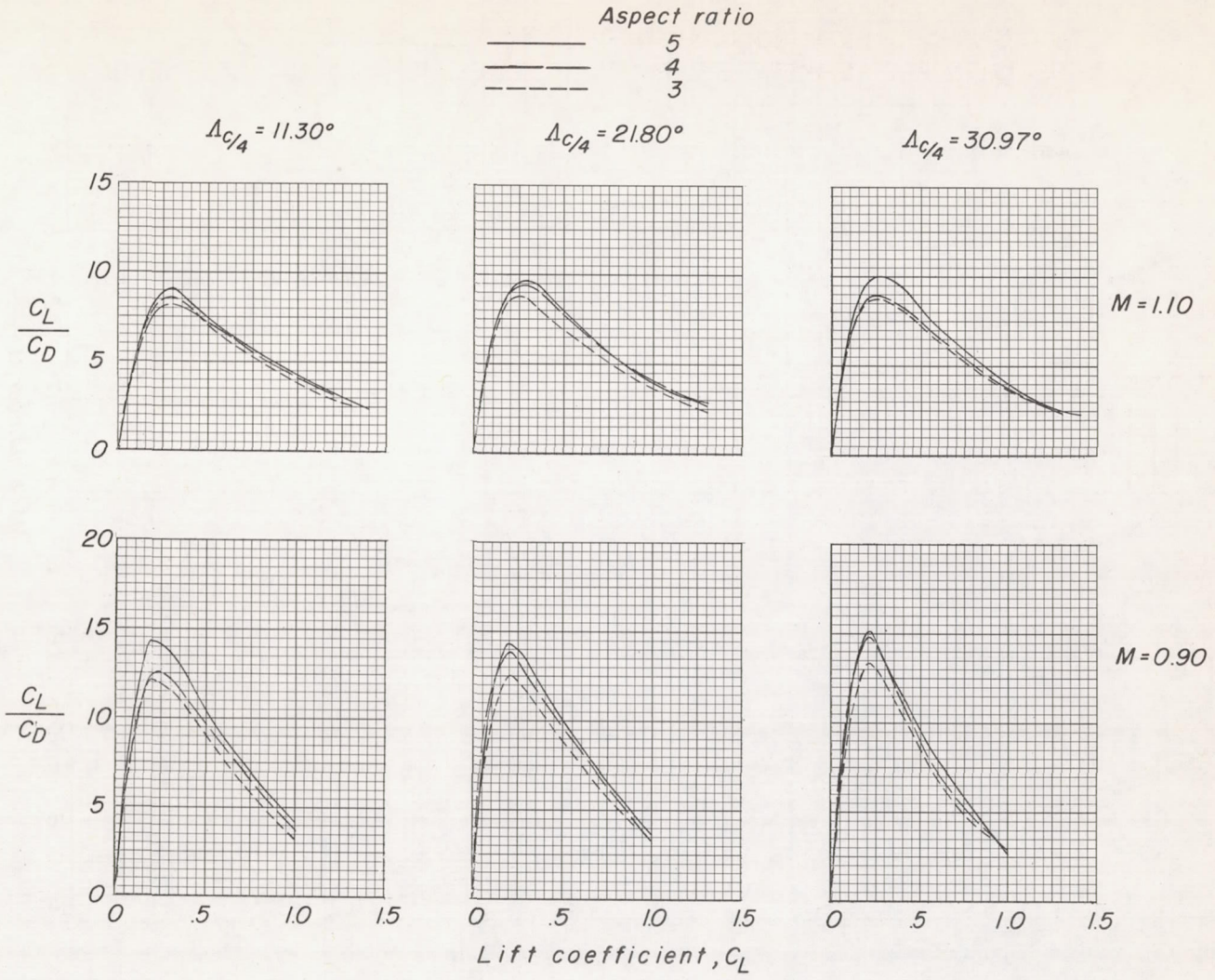


Figure 17.- Effect of aspect ratio and sweep on the variation of lift-drag ratios with lift coefficient.

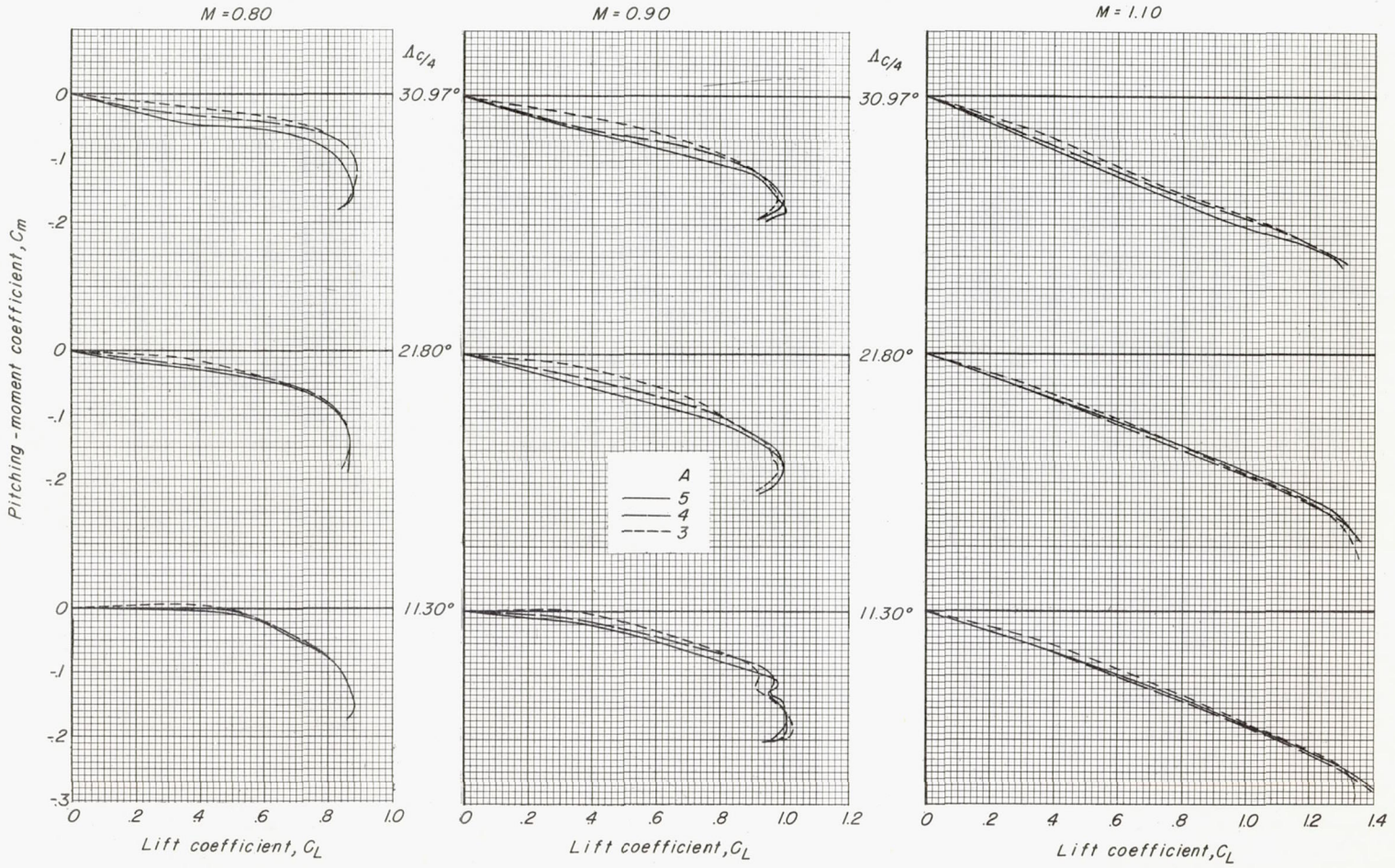


Figure 18.- Effect of aspect ratio and sweep on the variation of pitching-moment coefficient with lift coefficient.

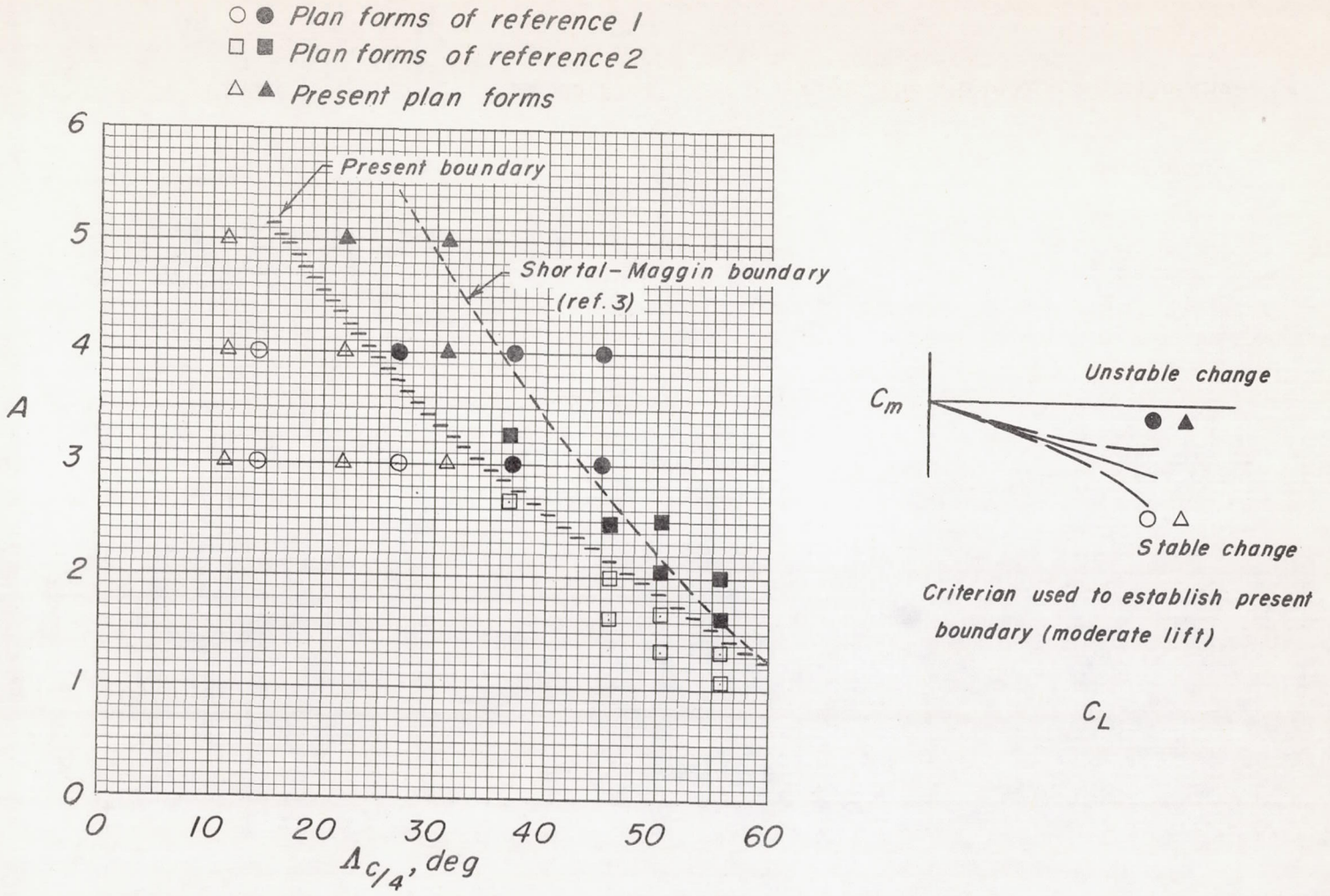


Figure 19.- Boundary separating highly tapered plan forms that become increasingly stable with increasing lift from those that become decreasingly stable with increasing lift.

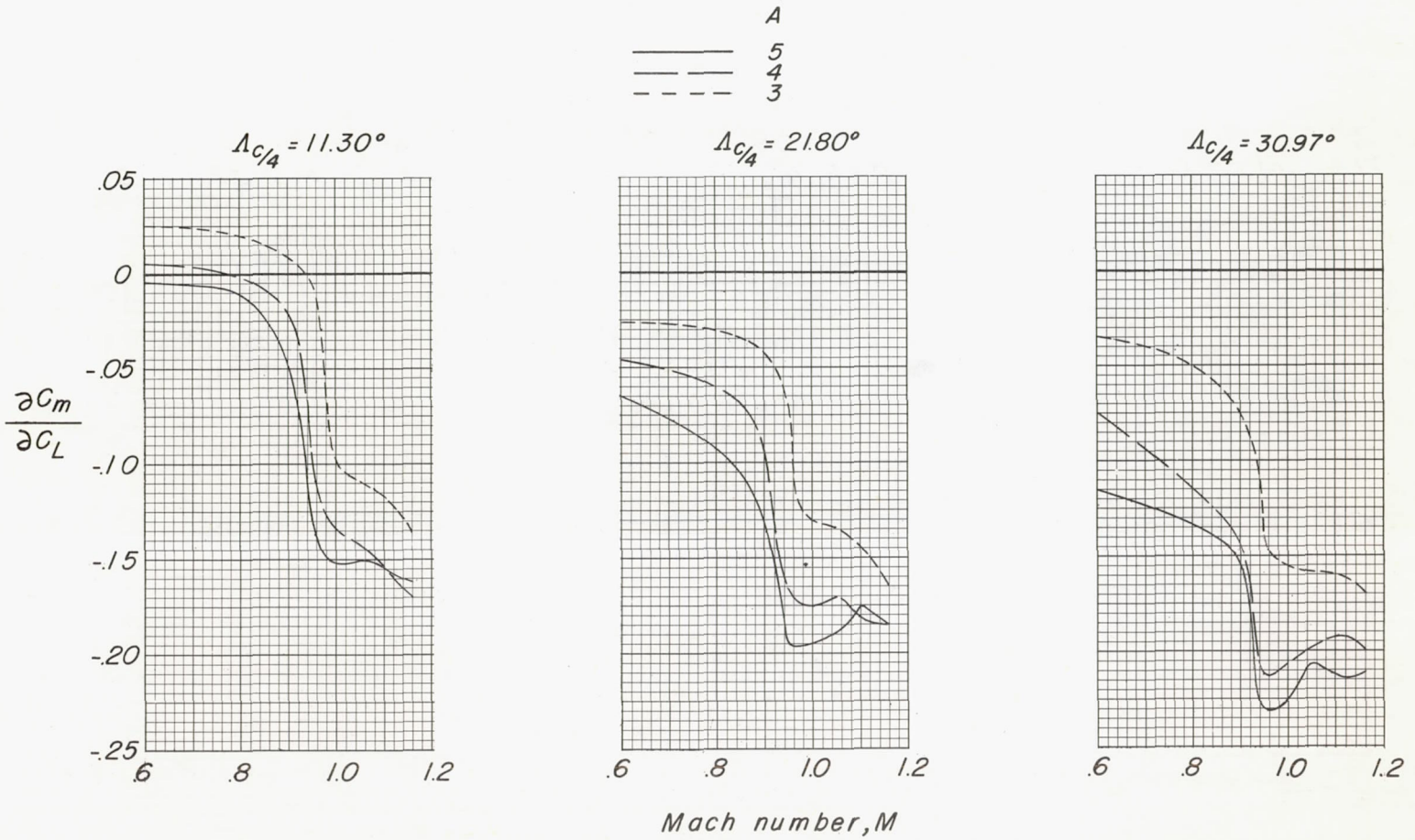
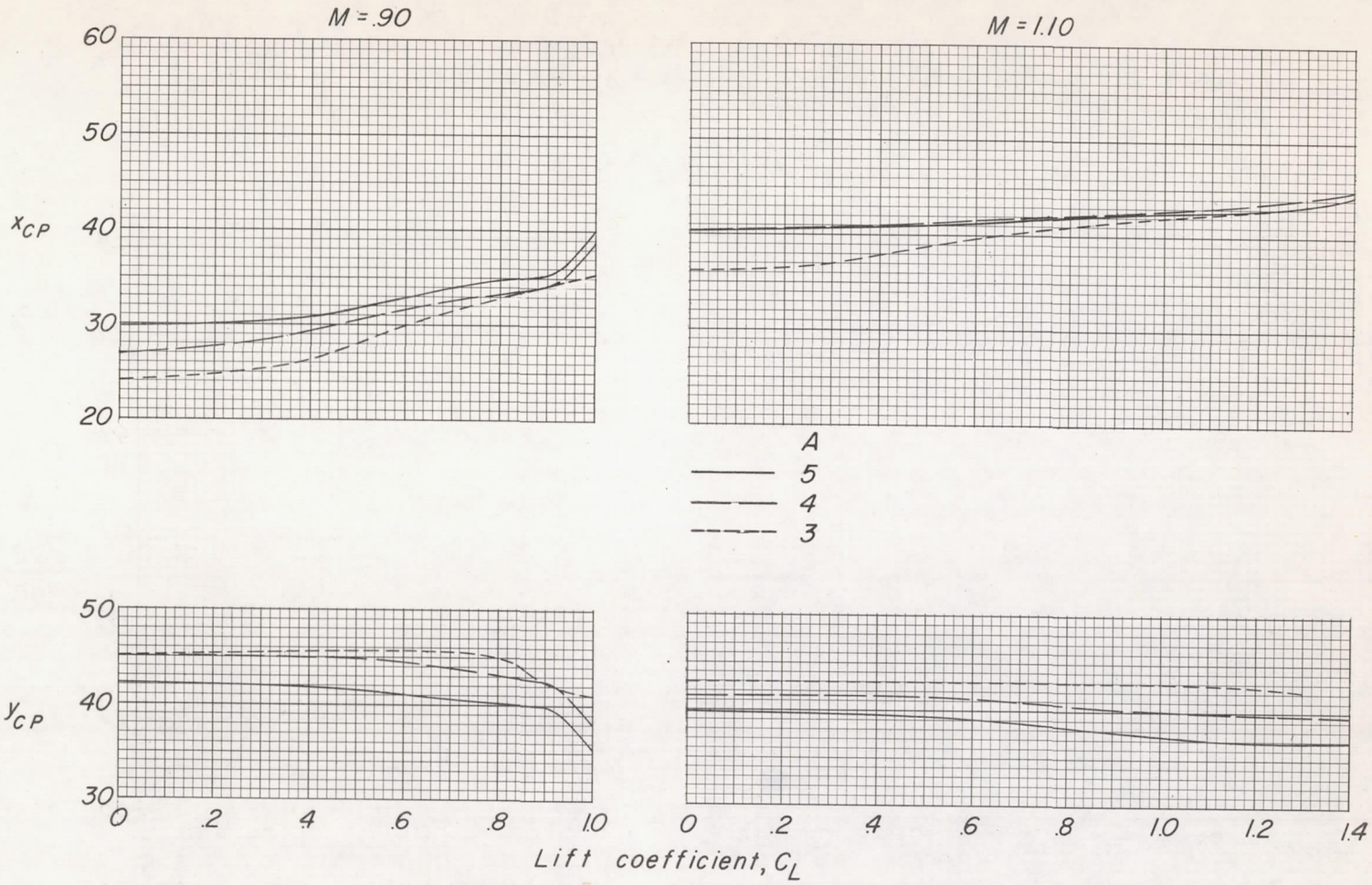
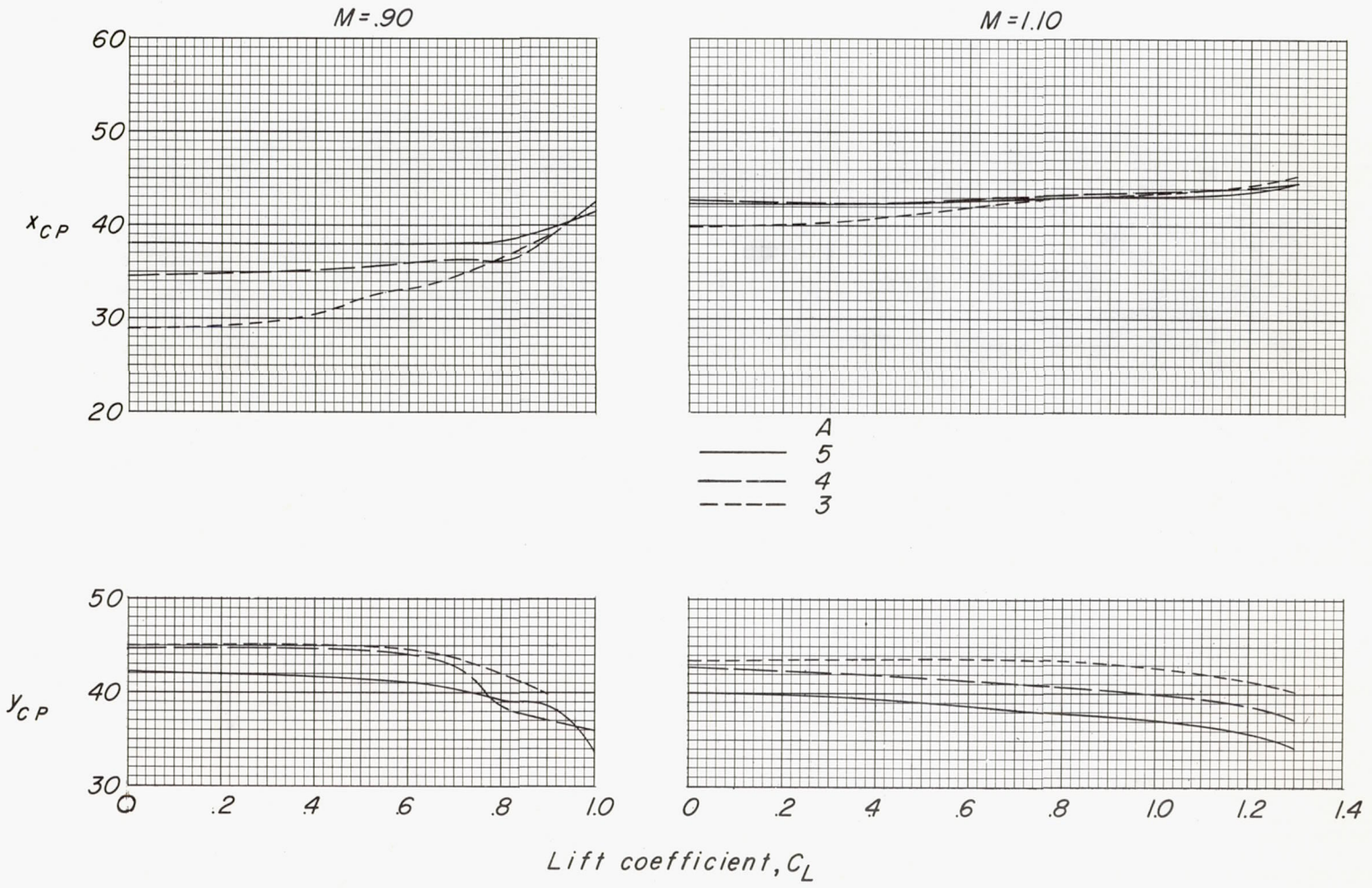


Figure 20.- Effect of aspect ratio and sweep on the variation of aerodynamic center with Mach number.



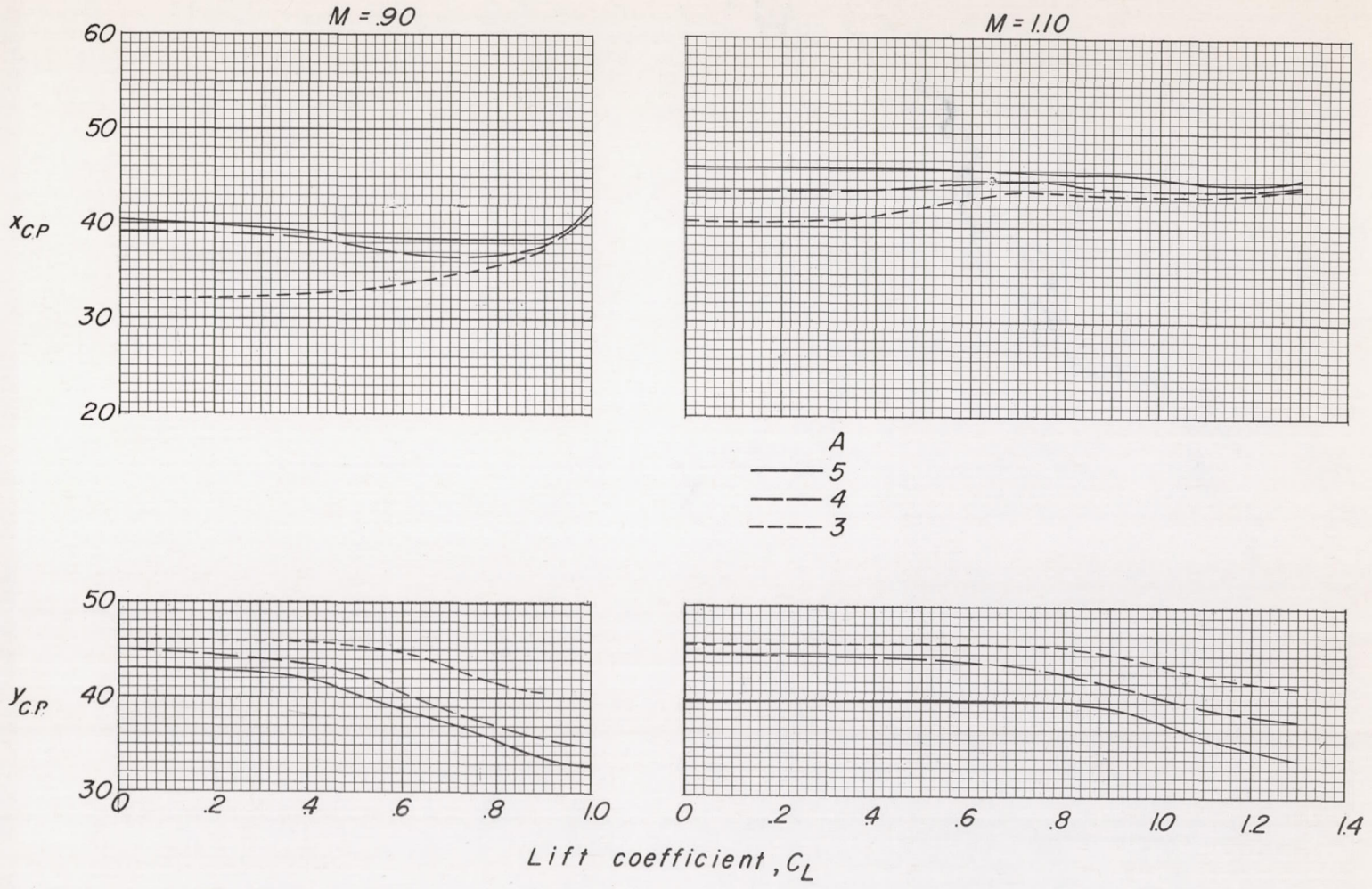
(a) $\Lambda_{c/4} = 11.30^{\circ}$.

Figure 21.- Effect of aspect ratio and sweep on the variation of the effective center of pressure with lift coefficient.



(b) $\Lambda_{c/4} = 21.80°$.

Figure 21.- Continued.



(c) $\Lambda_{c/4} = 30.97^{\circ}$.

Figure 21.- Concluded.

NACA - Langley Field, Va.